

Spatial distribution of environmental indicators in surface sediments of Lake Bolshoe Toko, Yakutia, Russia

Boris K. Biskaborn^{1*}, Larisa Nazarova^{1,2,3}, Lyudmila A. Pestryakova⁴, Liudmila Syrykh⁵, Kim Funck^{1,6}, Hanno Meyer¹, Bernhard Chaplignin¹, Stuart Vyse¹, Ruslan Gorodnichev⁴, Evgenii Zakharov^{4,7}, Rong Wang⁸, Georg Schwamborn^{1,9}, Bernhard Diekmann^{1,2}

*Corresponding author's Email: boris.biskaborn@awi.de

1 Alfred Wegener Institute Helmholtz Centre for Polar and Marine Research, Potsdam, Germany

2 University of Potsdam, Potsdam, Germany

3 Kazan Federal University

4 North-Eastern Federal University of Yakutsk, Russia

5 Herzen State Pedagogical University of Russia, St. Petersburg, Russia

6 Humboldt University Berlin, Germany

7 Institute for Biological Problems of Cryolithozone Siberian Branch of RAS, Yakutsk, Russia

8 Key Laboratory of Submarine Geosciences, State Oceanic Administration, Hangzhou, China

9 Free University of Berlin, Berlin, Germany

Manuscript status:

Approved by all authors. English proofread.

Keywords:

Diatoms, chironomids, XRF elements, XRD minerals, grain-size distribution, oxygen isotopes, organic carbon

Abstract

Rapidly changing climate in the northern hemisphere and associated socio-economic impacts require reliable understanding of lake systems as important freshwater resources and sensitive sentinels of environmental changes. To better understand time-series data in lake sediment cores it is necessary to gain information on within-lake spatial variabilities of environmental indicator data. Therefore, we retrieved a set of 38 samples from the sediment surface along spatial habitat gradients in the boreal, deep, and yet pristine Lake Bolshoe Toko in southern Yakutia, Russia. Our methods comprise laboratory analyses of the sediments for multiple proxy parameters including diatom and chironomid **taxonomy**, oxygen isotopes from diatom silica, grain size distributions, elemental compositions (XRF), organic carbon contents, and mineralogy (XRD). We analysed the lake water for cations, anions and isotopes. Our results show that the diatom assemblages are strongly influenced by water depth and dominated by planktonic species, i.e.

43 *Pliocaenicus bolshetokoensis*. Species richness and diversity is higher in the
44 northern part of the lake basin, associated with the availability of benthic, i.e.
45 periphytic, niches in shallower waters. $\delta^{18}\text{O}_{\text{diatom}}$ values are higher in the deeper
46 south-western part of the lake probably related to water temperature differences.
47 The highest amount of the chironomid taxa underrepresented in the training set
48 used for palaeoclimate inference was found close to the Utuk river and at southern
49 littoral and profundal sites. Abiotic sediment components are not symmetrically
50 distributed in the lake basin but vary along restricted areas of differential
51 environmental forcings. Grain size and organic matter is mainly controlled by both,
52 river input and water depth. Mineral (XRD) data distributions are influenced by the
53 metamorphic lithology of the Stanovoy mountain range, while elements (XRF) are
54 intermingled due to catchment and diagenetic differences. We conclude that the
55 lake represents a suitable system for multiproxy environmental reconstruction based
56 on diatoms (including oxygen isotopes), chironomids and sediment-geochemical
57 parameters.

58
59

60 **1 Introduction**

61 Over the past few decades, the atmosphere in boreal and high elevation regions
62 has warmed faster than anywhere else on Earth (Pepin et al., 2015;Huang et al.,
63 2017). Dramatic socio-economic and ecological consequences are expected
64 (AMAP, 2017) as well as substantial feedbacks from thawing permafrost and
65 associated release of greenhouse gas in the global climate system (Schuur et al.,
66 2015). Boreal Russia, as compared to the rest of the world, has been reported as a
67 hot-spot region, where air temperature increases lead to substantial ground
68 warming over the last decade (Biskaborn et al., 2019). Estimations of the accurate
69 amplitude of environmental impact suffer from imprecise understanding of ecological
70 indicators of past environmental conditions (Miller et al., 2010). Lake ecosystems,
71 whose development is archived in their sediments, act as sensitive sentinels of
72 environmental changes (Adrian et al., 2009), but rely on careful interpretation of
73 suitable proxy data. Proxy information on present and past ecological conditions is
74 provided by various biological and physicochemical properties of the sediment
75 components (Meyer et al., 2015;Solovieva et al., 2015;Nazarova et al., 2017a).
76 However, the spatial within-lake distributions of preserved remnants of ecosystem
77 inhabitants and associated sediment-geochemical properties, depend on habitat
78 differences between the epilimnion and the hypolimnion (Raposeiro et al., 2018),
79 and are therefore expected to be non-uniform. Accordingly, precise
80 paleolimnological reconstruction of past environmental variability requires a
81 profound understanding of the recent within-lake heterogeneity.

82 Our approach comprises commonly applied sedimentological variables that help
83 to gain a holistic view on a lake's depositional history, including diatom and
84 chironomid **taxonomy**, $\delta^{18}\text{O}_{\text{diatom}}$, grain size distributions, elemental compositions,
85 organic carbon contents, and mineralogy. Abiotic sediment preferences represent
86 signals that result from external input of material and lake-internal conditions during
87 deposition as well as post-sedimentary diagenetic processes near the sediment
88 surface (Biskaborn et al., 2013b;Bouchard et al., 2016). To reliably identify true
89 environmental signals, it is therefore necessary to apply multiproxy approaches that
90 enable an understanding of lake-internal filters between original external forcing and
91 the resulting preferences of the sediment deposition (Cohen, 2003).

92 Diatoms (unicellular, siliceous microalgae) represent a major part of the aquatic
93 primary producers. They appear ubiquitous and their opaline frustules **are well**
94 **preserved** in the sedimentary record, allowing exact identification down to sub-
95 species level by high-resolution light microscope analysis (Battarbee et al., 2001).
96 Diatoms are among the most applied bioindicators for past and present ecosystem
97 changes in boreal environments (Miller et al., 2010;Pestryakova et al., 2012;Hoff et
98 al., 2015;Herzschuh et al., 2013;Biskaborn et al., 2012;Biskaborn et al.,
99 2016;Palagushkina et al., 2017;Douglas and Smol, 2010). Widespread responses of
100 planktonic diatoms to recent climate change prove that lakes in the northern
101 hemisphere often have already crossed important ecological thresholds (Smol and
102 Douglas, 2007;Rühland et al., 2008). The very rapid life cycles of the specimen of
103 days to weeks (Round et al., 1990) enables changes in diatom assemblages on
104 very short time-scales in response to changes in environmental circumstances, e.g.
105 cooling or warming (Anderson, 1990). The link between climate change and
106 diatoms, however, cannot easily be addressed via simple temperature-inference
107 models. The situation demands **a more complete understanding** of the interactions
108 between the aquatic ecosystem with lake habitat preferences, hydrodynamics and
109 catchment properties (Anderson, 2000;Palagushkina et al., 2012;Biskaborn et al.,
110 2016;Bracht-Flyr and Fritz, 2012;Hoff et al., 2015). **It is thus necessary to identify**
111 **the relationship between diatom species occurrence, the isotopic composition of**
112 **their opaline valves, and internal physico-limnological factors (Heinecke et al., 2017)**
113 **within spatial heterogenic lake systems before drawing direct inferences about**
114 **external climatic driven factors from single core studies.**

115 Chironomid larvae (Insecta: Diptera) can make up to 90% of the aquatic
116 secondary production (Herren et al., 2017;Nazarova et al., 2004) and hence their
117 preserved head capsules represent well the aquatic heterotrophic bottom-dwelling
118 ecosystem component (Nazarova et al., 2008;Syrykh et al., 2017;Brooks et al.,
119 2007). Furthermore, literature reports a net mutualism of chironomids and benthic
120 algae between the primary consumer and primary producer trophic levels in benthic
121 ecosystems (Specziar et al., 2018;Zinchenko et al., 2014). Factors influencing the

122 spatial distribution of chironomids within single lakes are water temperature
123 (Nazarova et al., 2011;Luoto and Ojala, 2018), sedimentological habitat
124 characteristics (Heling et al., 2018) and/or water depth and nutrients (Yang et al.,
125 2017), as well as hypolimnetic oxygen (Stief et al., 2005) and the availability of
126 water plants (Raposeiro et al., 2018;Wang et al., 2012b).

127 Secondary factors influencing the spatial distribution of subfossil assemblages
128 are selective transitions from living communities to accumulation of dead remains.
129 Both, biological remains and physico-chemical properties are influenced by
130 sediment resuspension and redistribution processes described as sediment
131 focusing (Hilton et al., 1986) which mainly depend on slope steepness (Hakanson,
132 1977) or, in shallow areas, wind-induced bottom shear stress (Bennion et al.,
133 2010;Yang et al., 2009). Nevertheless, it already has been proven for other lake
134 sites that within-lake bioindicator distributions are laterally non-uniform, contradicting
135 the assumption that mixing processes cause homogenous microfossil assemblages
136 before deposition (Anderson, 1990;Wolfe, 1996;Anderson et al., 1994;Earle et al.,
137 1988;Kingston et al., 1983;Puusepp and Punning, 2011;Stewart and Lamoureux,
138 2012;Yang et al., 2009). However, many palaeolimnological studies have hitherto
139 ignored that single-site approaches using only one sediment core do not encompass
140 the full spatial extent and natural variability of the entire lake sediment archive.
141 Heggen et al. (2012) reported that sediment cores from the deep centre of small and
142 shallow lakes with high spatial proxy variability in the littoral zones contain
143 representative bioindicator assemblages. The authors also conclude, that in larger
144 and deeper lakes similar multi-site studies are necessary to make recommendations
145 about the “ideal” coring positions for multi-proxy palaeolimnological studies.

146 In this respect, our general research question was: how spatially reliable are
147 palaeolimnological proxy data in a complex lake system? To answer this question,
148 we set up our research hypotheses: (1) Bioindicators will respond to different habitat
149 properties and hence vary spatially in a complex lake system. (2) Water depth and
150 sediment-geochemical parameters will correlate with species assemblages at
151 different locations within a lake basin.

152 An analysis of spatio-temporal within-lake bioindicator distribution requires a
153 suitable and large lake system with an anthropogenically untouched ecosystem and
154 sufficient variability in water depth, catchment setting, and the sedimentological
155 regime. These demands are met by Lake Bolshoe Toko which ~~was considered as~~
156 the deepest lake in Yakutia (Zhirkov et al., 2016), located in the Sakha Republic,
157 Russia (Fig. 1). Our study aims to gain a better local understanding of proxy data for
158 planned palaeoenvironmental analyses of long sediment cores from Bolshoe Toko.
159 Therefore, our objectives are (1) to detect the spatial variability of abiotic (elements,
160 minerals, grain size) and biotic (diatoms, chironomids, organic carbon) components
161 of the lake’s surface sediments, (2) to reveal the causal relationship between the

162 distribution of aquatic microfossils, lake basin features, and sedimentary
163 parameters, and (3) to attribute proxy variability to stressors and factors of the lake
164 basin and its catchment.

165

166 2 Study site

167 The maximum diameter of Lake Bolshoe Toko (56°15'N, 130°30'E, 903 m.a.s.l) is
168 15.4 km, the maximum width is 7.6 km, the maximum water depth is 78 m (average
169 30.5 m), the surface area 8500 Ha, and the water transparency is 9.8 m and the
170 lake was indexed as “clean oligotrophic water” (Zhirkov et al., 2016). The north
171 eastern lake basin is shallower (<30 m) compared to the south western part of the
172 lake (up to 80 m). The Utuk river runs through Lake Maloe Toko and brings water
173 from the southern igneous catchment. The Lake Maloe Toko (called “small Toko”,
174 size 2.7 x 0.9 km, 168 m depth, tectonic origin) is located between high mountains
175 south of Bolshoe Toko. The river inflow south of Bolshoe Toko forms deltaic
176 sediments. The bay in the southeast is called Zaliv Rybachi (‘‘Fishing bay’’). It is
177 partly separated from the main basin and supplied with water by a small creek that
178 itself is connected to a small lake (Fig. 1). The bay is reported to have a somewhat
179 different fauna as compared to the Bolshoe Toko main basin, i.e. occurrence of fish
180 that is typical for small lakes and not found out of the basin (Semenov, 2018). The
181 ‘‘Banya lake’’ in the northeast is completely separated from Bolshoe Toko and was
182 hence not considered in this study. The Mulam river is the lake’s predominant
183 outflow towards the northern direction along the south eastern border of Yakutia
184 flowing into the Uchur, Aldan and finally into the Lena rivers.

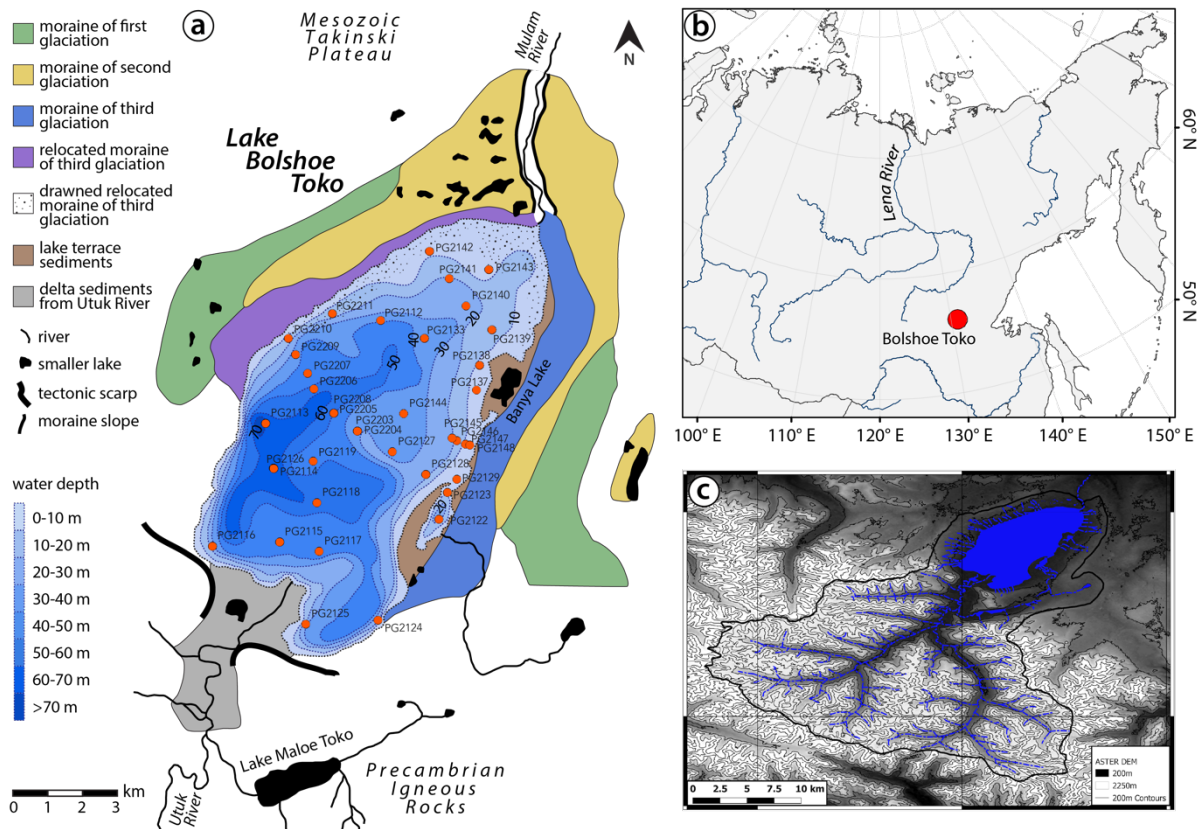
185 There are no permanent settlements in the study area. During the time of field
186 work there was a temporary mining settlement (built in 2011) located 17 km
187 northwest from Bolshoe Toko in the upper course of the Elga river. This settlement
188 was accessible by off-road vehicles we used to reach the lake, partly along
189 temporary winter roads (frozen rivers and lakes) in March 2013. The exploitation of
190 the El’ginsky coal deposits, planned for a productivity of 15-20 million tons year⁻¹
191 (Konstantinov, 2000), will strongly affect the lake and its catchment. The territory of
192 the watershed will increasingly be damaged and contaminated by off road vehicles
193 and rain fall will produce muddy water which potentially can cause lake pollution
194 (Sobakina and Solomonov, 2013).

195 The lake basin is adjoined to the northern slope of the eastern Stanovoy
196 mountain range in a depression of tectonic and glacial origin between two
197 northwest-trending right-lateral strike-slip faults (Imaeva et al., 2009). A southward
198 thrust fault runs along the southern border of the lake separating the Precambrian
199 igneous rocks in the south from sandstones and mudstones of the Mesozoic
200 Tokinski Plateau in the north. The Stanovoy mountain range in the southern

201 catchment of the lake consists mainly of highly mafic granulites and other high-
202 pressure metamorphic rock types (Rundqvist and Mitrofanov, 1993). At its north-
203 eastern margins the lake is bordered by moraines of three different glacial sub-
204 periods (Kornilov, 1962) (Fig. 2).

205 The study area is situated within the East Siberian continental temperate climate
206 zone exhibiting taiga vegetation (boreal forests) and fragments of steppes and a
207 predominant westerly wind system (Shahgedanova, 2002). The meteorological
208 station in Yakutsk has recorded historical climate data (Gavrilova, 1993). In the 19th
209 Century the mean annual temperature was circa -11° to -11.5°C. During the 20th
210 Century temperatures have increased to around -10.2°C, in parallel with an increase
211 in precipitation from 205 to 250 mm per year. The meteorological station “Toko”
212 located approximately 10 km northeast of the lake, however, recorded mean annual
213 air temperatures of -11.2°C (January min. -65°C, July max. +34°C, annual
214 precipitation 276-579 mm). Measurements taken directly at the lake were lower,
215 indicating the influence of cold water from the Stanovoy mountain range in summer
216 and the high volume of ice during wintertime (Konstantinov, 2000). Since the
217 average air temperature in southern Yakutia increases with height (temperature
218 inversion of ~2°C 100 m⁻¹), permafrost can be locally discontinuous where taliks
219 (unfrozen zones) underneath topographically high and deep lakes penetrate the
220 permafrost zone (Konstantinov, 1986). As observed in 1971 (Konstantinov, 2000)
221 ice cover lasts at least partly until mid-July.

222
223
224



225
226
227
228
229
230
231
232
233
234
235

Fig. 1 Lake Bolshoe Toko study site. **a** Geological map, bathymetry and moraines. Map compiled using data from Konstantinov (2000) and Kornilov (1962). **b** Overview map of Siberia. World Borders data are derived from http://thematicmapping.org/downloads/world_borders.php and licensed under CC BY-SA 3.0. **c** Catchment area around Bolshoe Toko delineated from the ASTER GDEM V2 model between the latitudes N54° and N56° and longitudes E130° to E131° (1) (Meyer et al., 2011) and a corresponding multispectral Landsat 8 OLI TIRS satellite image using QGIS (QGIS-Team, 2016). Most of the river catchment is located in the igneous Precambrian Stanovoy mountain range supplying the southern part of the lake with water and sediment. The shallower northeastern part of the lake is influenced by the surrounding moraines and Mesozoic sand- and mudstones.

236 **3 Materials and methods**

237 **3.1 Field work**

238 Field work was conducted during the German-Russian expedition “Yakutia 2013”
239 between March 19th to April 14th 2013 by the Alfred Wegener Institute Helmholtz
240 Centre for Polar and Marine Research (AWI) and the North Eastern Federal State
241 University in Yakutsk (NEFU). Lake basin bathymetry was measured with a portable
242 **Echo Sounder**. Water samples for hydrochemical analyses of the water column and
243 the ice layer were collected prior to sediment coring using a UWITEC water
244 sampler. Water samples were analysed in situ using a WTW Multilab 340i for pH,
245 conductivity, and oxygen values at the day of retrieval during field work. A sub-
246 sample of the original water was passed through a 0.45 µm cellulose-acetate filter,
247 stored and transported in 60-ml Nalgene polyethylene bottles for subsequent anion

248 and cation analyses in AWI laboratories in autumn 2013. Cation samples were
249 acidified during field work with HNO₃, suprapure (65%) to prevent microbial
250 conversion processes and adsorptive accretion.

251 At 42 sites within the lake, short cores containing intact sediment surface material
252 were retrieved using an UWITEC gravity corer. Water depth at sampling sites was
253 measured using either a hand-held HONDEX PS-7 LCD digital sounder and/or the
254 cord of the coring device when the lake ice cover disturbed the signal. The sediment
255 was identified as clayish silt deposits with predominant dark (black) color and a
256 weak smell of hydrogen sulphide, a sticky and viscous mud mixed with plant and
257 other organic residues. The uppermost ca. 2 cm at some sites had a dark red
258 colouring indicating the redox boundary between oxygenated and anoxic sediments.
259 We identified the uppermost 0.5 cm of short cores as surface sediments and
260 subsampled these layers onsite during fieldwork to avoid sediment mixture during
261 transport. Sediment samples were transported in sterile "Whirl-Pak" bags and
262 sediment cores were transported in plastic liners to the AWI laboratories in
263 Potsdam, Germany, and stored at 4°C in a dark room for further analyses and as
264 back-up.

265 **3.2 Laboratory analyses**

266 **3.2.1 Hydrochemistry**

267 From the water samples, anions were analysed using ion chromatography
268 (Dionex DX 320) and cations were determined using inductively coupled plasma–
269 optical emission spectrometry (ICP-OES, Perkin-Elmer Optima 8300DV Perkin-
270 Elmer – Optical Emission Spectrometer. Hydrogen carbonate concentrations were
271 measured by titration with 0.01 M HCl using an automatic titrator (Metrohm 794
272 Basic Titrino).

273 Stable hydrogen and oxygen isotope analyses were carried out with Finnigan
274 MAT Delta-S mass spectrometers with two equilibration units using common
275 equilibration techniques (Meyer et al., 2000), and given as $\delta^{18}\text{O}$ and δD in ‰ vs.
276 VSMOW (Vienna Standard Mean Ocean Water). The d excess ($d = \delta\text{D} - 8\delta^{18}\text{O}$) is
277 indicative for evaporation conditions in the moisture source region (Dansgaard,
278 1964; Merlivat and Jouzel, 1979).

279 **3.2.2 X-ray fluorescence and X-ray diffractometry**

280 The elemental composition of 20 freeze-dried and milled surface samples was semi-
281 quantitatively analysed by X-ray fluorescence (XRF) using a novel single sample
282 modification for the AVAATECH XRF core scanner at AWI Bremerhaven. A
283 Rhodium X-ray tube was warmed up to 1.75mA and 3 mA with a detector count time
284 of 10s and 15s for elemental analysis at 10kV (No filter) and 30kV (Pd-Thin filter)

285 respectively. The average modelled chi square values (χ^2) of measured peak
286 intensity curve fitting for the relevant elements were variable, but generally low (Zr =
287 0.92, Mn = 1.49, Fe = 2.32, Ti = 1.53, Br = 3.65, Sr = 4.79, Rb = 4.98, Si = 16.11).
288 Values above 3 were ascribed to suspiciously high count rates from sample PG2133
289 which was subsequently excluded from XRF interpretation. The relatively low
290 amount of total sample material available did not facilitate the removal of organic
291 matter before prior to sample measurement and may have contributed to the
292 variable modelled chi square values.

293 As interpretation of raw device obtained element intensities (in counts per second,
294 cps) is problematic due to non-linear matrix effects and variations in sample density,
295 water content and grain-size (Tjallingii et al., 2007), cps values were transformed
296 using a centred-log ratio transformation (CLR). Element ratios were calculated from
297 raw cps values and transformed using an additive-log ratio transformation (ALR)
298 (Weltje and Tjallingii, 2008).

299 The mineralogical composition of 32 freeze-dried and milled samples was
300 analysed by standard X-ray diffractometry (XRD) using a Philips PW1820
301 goniometer at AWI Bremerhaven applying Cobalt-Potassium alpha (CoK α) radiation
302 (40 kV, 40 mA) as outlined in Petschick et al. (1996). The intensity of diffracted
303 radiation was calculated as counts of peak areas using XRD processing software
304 MacDiff 4.0.7 (freeware developed by R. Petschick in 1999). Individual mineral
305 contents were expressed as percentages of bulk sediment XRD counts (Voigt,
306 2009). Mineral inspection focused on quartz, plagioclase and K-feldspar,
307 hornblende, mica, and pyrite. Clay minerals involved kaolinite, smectite and chlorite.
308 Accuracy of the semi-quantitative XRD method is estimated to be between 5 and
309 10% (Gingele et al., 2001).

310

311 **3.2.3 Grain-size, carbon and nitrogen analyses**

312 In order to gain high-resolution information on the grain-size distribution, organic
313 material was removed from 32 surface sediment samples by hydrogen peroxide
314 oxidation over four weeks on a platform shaker. Two homogenised subsamples
315 were weighted and 93 subclasses between 0.375 and 2000 μm were measured
316 using a Coulter LS 200 Laser Diffraction Particle Analyser. Grain-size fractions
317 coarser than 2 mm were sieved out, weighted and added to the volume percentage
318 data afterwards to indicate the proportion of gravel.

319 Total carbon (TC) and total nitrogen (TN) of 35 freeze-dried and milled samples
320 was quantified by heating the material in small tin capsules using a Vario EL III CNS
321 analyser and total organic carbon (TOC) was measured using a Vario MAX C in per
322 cent by weight (wt%). The measurement accuracy was 0.1 wt% for TOC and TN,
323 and 0.05 wt% for TC. TOC and TN were compared to calculate the TOC/TN_{atomic}

324 ratio by multiplying with the ratio of atomic weights of nitrogen and carbon following
325 Meyers and Teranes (2002).

326 The stable carbon isotope composition $\delta^{13}\text{C}$ of the total organic carbon fraction
327 was measured in 15 samples using a Finnigan Delta-S mass spectrometer. Dried,
328 milled and carbonate-free (HCl treated) samples were combusted in tin capsules to
329 CO_2 . Results are expressed as $\delta^{13}\text{C}$ values relative to the PDB standard in parts per
330 thousand (‰) with an error of $\pm 0.15\%$.

331 3.2.4 Diatoms

332 23 samples were prepared for diatom analysis following the standard procedure
333 described by Battarbee et al. (2001). To calculate the diatom valve concentration
334 (DVC) 5×10^6 microspheres were added to each sample following organic removal
335 with hydrogen peroxide. Diatom slides were prepared on a hot plate using Naphrax
336 mounting medium. For the identification of diatoms to the lowest possible taxonomic
337 level we used several diatom flora including Lange-Bertalot et al. (2011), Lange-
338 Bertalot and Metzeltin (1996), Krammer and Lange-Bertalot (1986-1991) and
339 Lange-Bertalot and Genkal (1999). For rare taxa (i.e. *Pliocaenicus*) literature
340 research was applied in scientific papers, including Cremer and Van de Vijver
341 (2006) and Genkal et al. (2018). A minimum of 300 (and up to 400) diatom valves
342 were counted in each sample using a Zeiss AXIO Scope.A1 light microscope with a
343 Plan-Apochromat 100 \times /1.4 Oil Ph3 objective at 1000x magnification. Identification of
344 small diatom species was verified using a scanning electron microscope (SEM) at
345 the GeoForschungsZentrum Potsdam.

346 During counting of diatom valves, chrysophycean stomatocysts and *Mallomonas*
347 were counted but not further taxonomically identified. Count numbers were used to
348 estimate the chrysophyte cyst to diatom index (C:D) and *Mallomonas* to diatom
349 index (M:D) relative to counted diatom cells (Smol, 1984; Smol and Boucherle,
350 1985).

351

352 3.2.5 Oxygen isotopes of diatom silica

353 To analyze the oxygen isotope composition from diatom silica ($\delta^{18}\text{O}_{\text{diatom}}$) from 9
354 representative surface samples, a purification procedure including wet chemistry (to
355 remove organic matter and carbonates) and heavy liquid separation was applied for
356 the fraction $<10 \mu\text{m}$ following the method described in Chaplignin et al. (2012). After
357 freeze-drying the samples were treated with H_2O_2 (32%) and HCl (10%) to remove
358 organic matter and carbonates and wet sieved into $<10 \mu\text{m}$ and $>10 \mu\text{m}$ fractions.
359 Four multiple heavy liquid separation (HLS) steps with varying densities (from 2.25
360 to 2.15 g/cm^3) were then applied using a sodium polytungstate (SPT) solution

361 before being exposed to a mixture of HClO₄ (65%) and HNO₃ (65%) for removing
362 any remaining micro-organics.

363 To remove exchangeable hydrous groups from the diatom valve structure
364 (amorphous silica SiO₂ * nH₂O), inert Gas Flow Dehydration was performed
365 (Chapligin et al., 2010). Oxygen isotope analyses were performed on dehydrated
366 samples using laser fluorination technique (with BrF₅ as reagent to liberate O₂) and
367 then directly measured against an oxygen reference of known isotopic composition
368 using a PDZ Europa 2020 mass spectrometer (MS2020, now supplied by Sercon
369 Ltd., UK). The long-term analytical reproducibility (1σ) is ±0.25 ‰ (Chapligin et al.,
370 2010).

371 Every fifth sample was a biogenic working standard to verify the quality of the
372 analyses. For this, the biogenic working standard BFC calibrated within an inter-
373 laboratory comparison was used (Chapligin, 2011). With a δ¹⁸O value of +29.0±0.3
374 ‰ (1σ) BFC (this study: +28.7±0.17 ‰, n=49) is the closest diatom working
375 standard to the Bolshoe Toko samples (δ¹⁸O values range between +22 and +24 ‰)
376 available. A contamination correction was applied to δ¹⁸O_{diatom} using a geochemical
377 mass-balance approach (Chapligin et al., 2012;Swann et al., 2007) determining the
378 contamination end-member by analysing the heavy fractions after the first heavy
379 liquid separation resulting in Al₂O₃=16.2±1.3 % (via EDX; n=9) and δ¹⁸O=8.5±0.8 ‰
380 (n=6).

381 **3.2.6 Chironomids**

382 Treatment of 18 sediment samples for chironomid analysis followed standard
383 techniques described in Brooks et al. (2007). Subsamples of wet sediments were
384 deflocculated in 10 % KOH, heated to 70 °C for up to 10 minutes, to which boiling
385 water was added and left to stand for up to another 20 minutes. The sediment was
386 passed through stacked 225 and 90 μm sieves. Chironomid larval head capsules
387 were picked out of a grooved Bogorov sorting tray under a stereomicroscope at 25-
388 40x magnifications and were mounted in Hydromatrix two at a time, ventral side up,
389 under a 6 mm diameter cover slip. From 48 to 117 chironomid larval head capsules
390 were extracted from each sample, to capture the maximum diversity of the
391 chironomid population. Chironomids were identified to the highest taxonomic
392 resolution possible with reference to Wiederholm (1983) and Brooks et al. (2007).
393 Information on the ecology of chironomid taxa and groups was taken from Brooks et
394 al. (2007), Pillot (2009) and Nazarova et al., (2011;2015;2008;2017b)). Ecological
395 information of the taxa associated to biotopes (littoral, profundal), water velocity
396 (standing, running water), and relation to presence of macrophytes were taken from
397 Brooks et al. (2007) and Pillot (2009). T July optima of chironomids were taken from
398 Far East (FE) chironomid-based temperature inference model (Nazarova et al.,
399 2015). The Far East (FE) chironomid-based temperature inference model (WA-PLS,

400 2 components; r^2 boot = 0.81; RMSEP boot = 1.43 °C) was established from a
401 modern calibration data set of 88 lakes and 135 taxa from the Russian Far East
402 (53–75°N, 141–163°E, T July range 1.8 – 13.3 °C). Mean July air temperature for
403 the lakes from the calibration data set was derived from (New et al., 2002). All
404 modern and chironomid-inferred temperatures were corrected to 0 m.a.s.l. using a
405 modern July air temperature lapse rate of 6 °C km⁻¹ (Livingstone et al., 1999;Heiri et
406 al., 2014).

407 **3.3 Statistical analyses**

408 Species richness and the Simpson diversity on diatom and chironomid data were
409 estimated after sample-size normalization using a rarefaction analysis in the iNext
410 package in R. Diatom valve preservation was measured and calculated as the f-
411 index (Ryves et al., 2001). Diatom valve concentration was estimated as the number
412 of valves per gram dry sediment following Battarbee and Kneen (1982).

413 Detrended Correspondence Analysis (DCA) with detrending by segments was
414 performed on the chironomid and diatom data (rare taxa downweighted) to
415 determine the lengths of the sampled environmental gradients, from which we
416 decided whether unimodal or linear statistical techniques would be the most
417 appropriate for the data analysis (Birks, 1995). For diatom data the gradient lengths
418 of the species scores were 2.07 and 1.49 standard deviation units (SDU) for DCA 1
419 and 2, respectively, suggesting that lineal numerical methods should be used. A
420 Principal Component Analysis (PCA) was used to explore the main taxonomic
421 variation of the data (ter Braak and Prentice, 1988). The gradient lengths of
422 chironomid species scores were 3.78 and 4.12 SDU indicating that numerical
423 methods based on a unimodal response model should be more appropriate to
424 assess the variation structure of the chironomid assemblages (ter Braak, 1995).
425 However, test PCA performed on chironomid data showed that lineal method
426 captures more variance of species data (ESM, Table a) therefore we further applied
427 lineal methods for both, chironomid and diatom data. In order to summarize the
428 response of lacustrine biota to abiotic, physicochemical explanatory variables, a
429 redundancy analysis (RDA) was performed on diatom and chironomid data in
430 comparison to environmental variables (Fig. 2 and 3).

431 Initially, all environmental variables shown in the Table 1 were used in RDA to
432 assess the relationships between the distribution of bioindicator taxa and abiotic
433 habitat parameters. Additionally we include in the analysis the presence/absence of
434 the submerged vegetation, distances of the sampling stations from the shore and
435 from the inflowing rivers. Variance inflation factors (VIF) were used to identify
436 intercorrelated variables. Environmental variables with a VIF greater than 20 were
437 eliminated, beginning with the variable with the largest inflation factor, until all
438 remaining variables had values < 20 (ter Braak and Smilauer, 2012). A set of RDAs

439 was performed on chironomid and diatom data with each environmental variable as
440 the sole constraining variable. The percentage of the variance explained by each
441 variable was calculated and statistical significance of each variable was tested by a
442 Monte Carlo permutation test with 999 unrestricted permutations. Significant
443 variables ($P \leq 0.05$) were retained for further analysis.

444 DCA, PCA and RDA were performed using CANOCO 5.04 (ter Braak and
445 Smilauer, 2012).

446 Percentage abundances of the chironomid taxa that are absent or rare in the
447 modern calibration data set were calculated at each sampling site in order to see the
448 distribution of the taxa that could potentially hamper a T July reconstruction in case
449 of palaeoclimatic study that could be done at each of the sampling sites. It is known
450 that less reliability should be placed on the samples in which more than 5% of the
451 taxa are not represented in the modern calibration data or more than 5% of the taxa
452 are rare in the modern calibration dataset (i.e. Hill's N_2 less than 5) (Heiri and Lotter,
453 2001;Self et al., 2011).

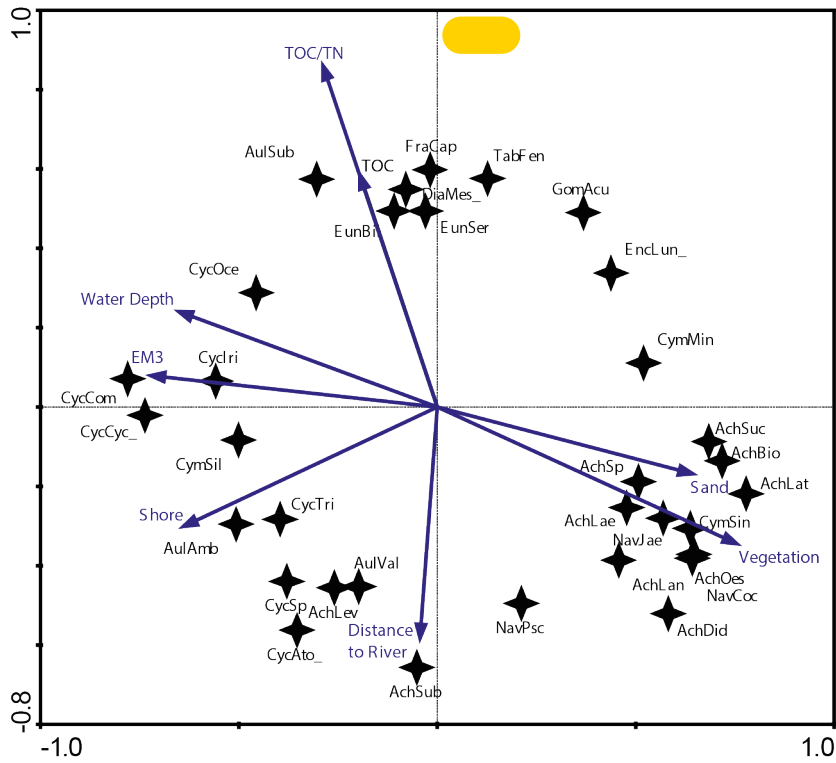
454 To assess the relative contribution of different sedimentary processes to the bulk
455 sediment, such as fluvial or aeolian transport (Wang et al., 2015;Biskaborn et al.,
456 2013b) a statistical end-member analysis on grain-size data was performed using
457 the MATLAB modelling algorithm of Dietze et al. (2012). In this method, individual
458 grain-size populations identified as end-member loadings (vol%, Fig. 4) as well as
459 their contributions to the bulk composition identified as scores (%) were derived by
460 eigenspace analysis, weight transformation, Varimax rotations and different scaling
461 procedures.

462 A Pearson correlation matrix of the main important variables (Fig. 5) was
463 calculated using the basic R core (R Core Team, 2012) and plotted using *corrplot*. A
464 p-value adjustment was applied to only assign colours to values that revealed p
465 < 0.05 . To identify the pattern, the correlation matrix was reordered according to the
466 correlation coefficient. Exceptional sites within the heterogenic lake system lead to
467 disturbance of good correlation coefficients within areas along natural borders, e.g.
468 water depth isobaths.

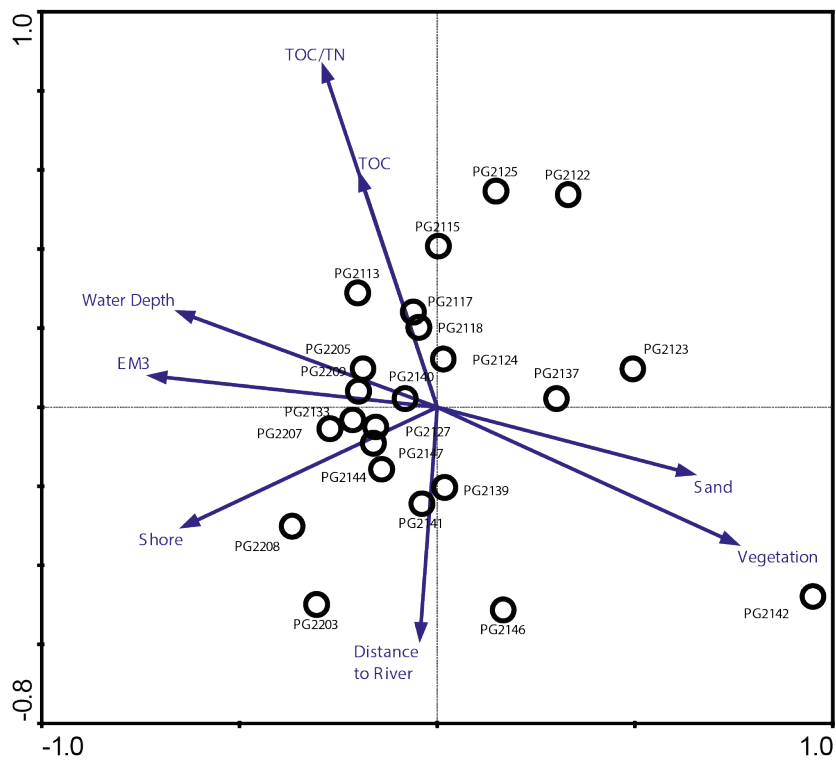
469 To guarantee the sustained availability of our research (Elger et al., 2016), the
470 data is uploaded and freely accessible in the PANGAEA repository (DOI: XXXXXX
471 will be provided during review process XXXXXXXX).

472
473

a. RDA, diatom species scores

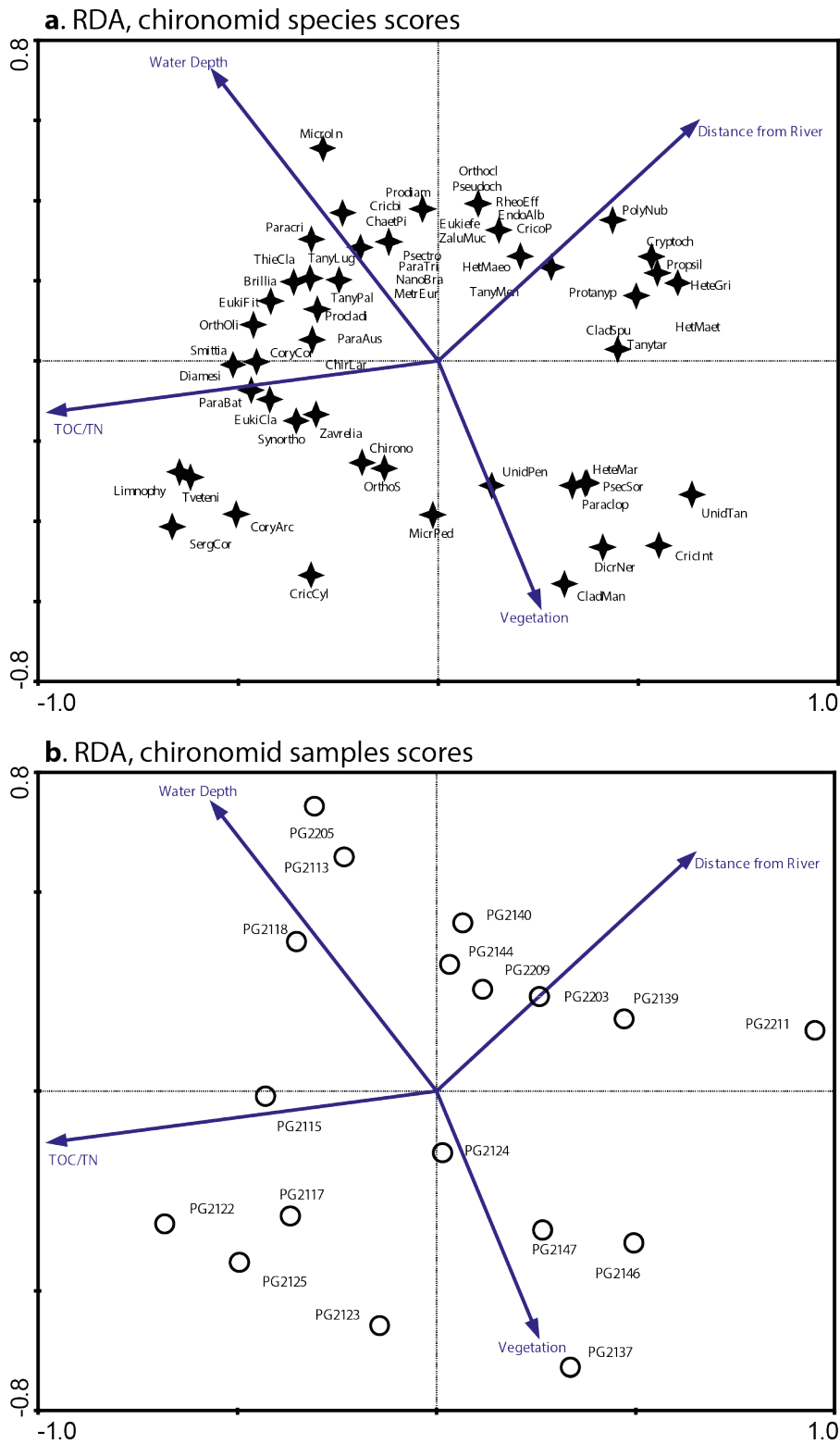


b. RDA, diatom samples scores

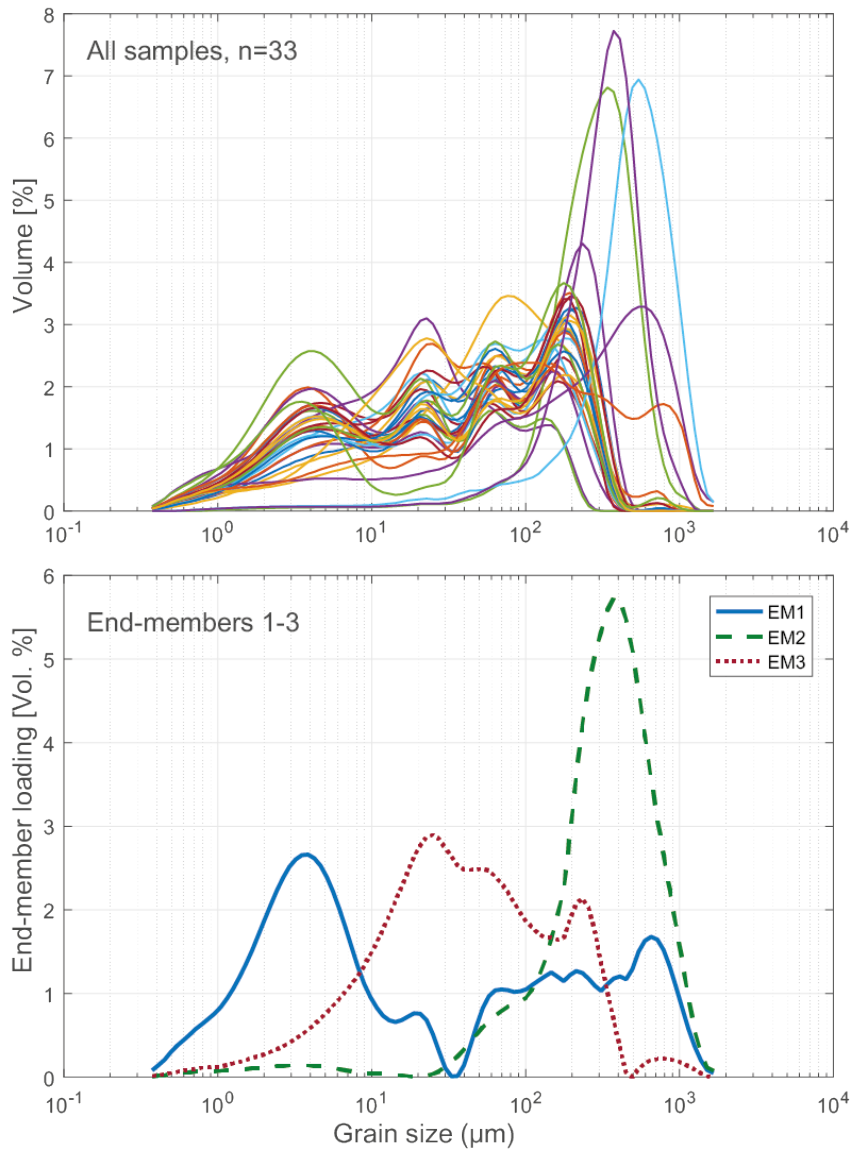


474
475
476
477
478
479

Fig. 2 RDA biplots of diatoms in the surface sediments of Lake Bolshoe Toko. (a) Common diatom taxa and significant environmental variables. (b) Diatom sampling sites and significant environmental variables.

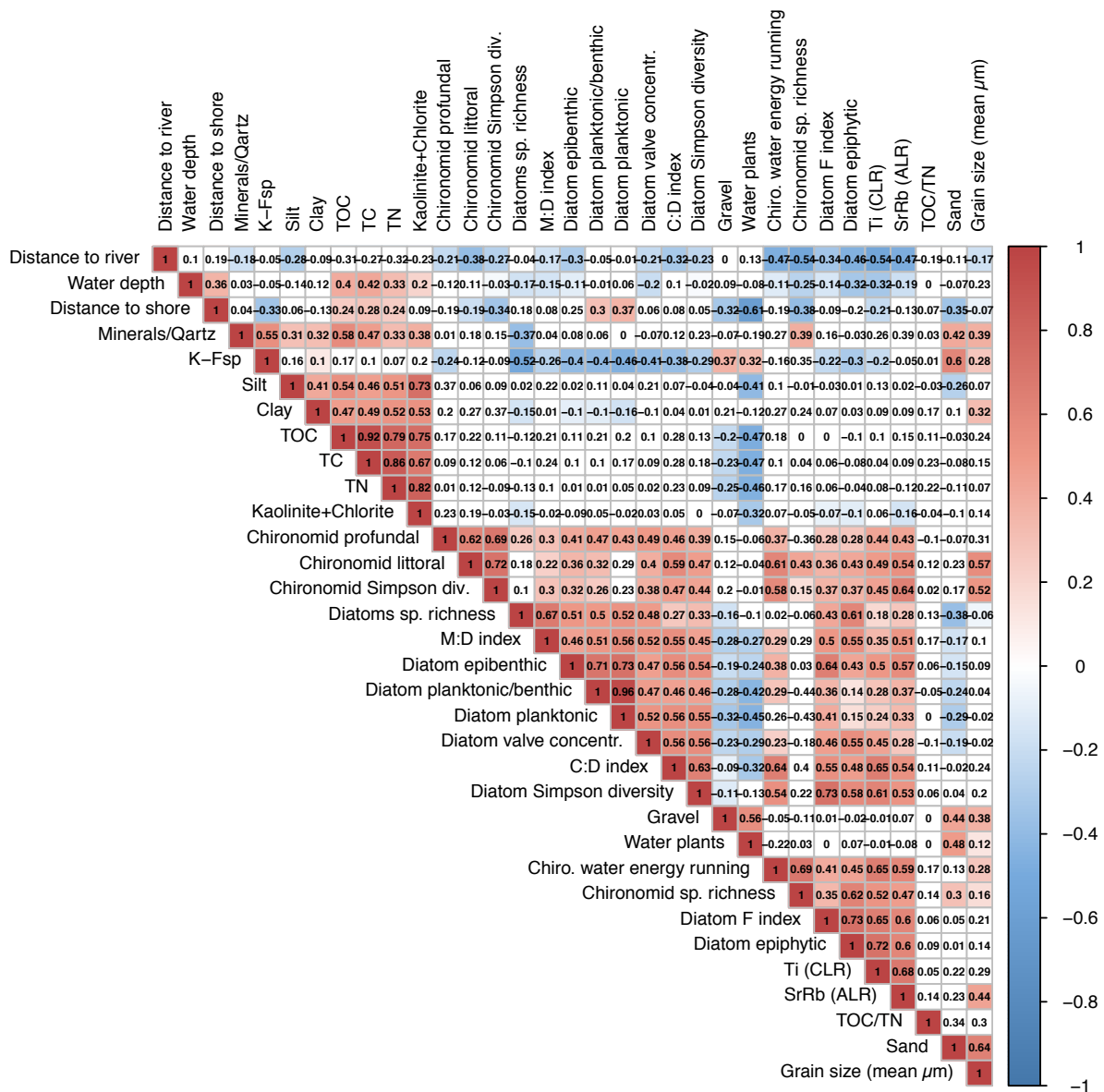


481
 482 **Fig. 2** RDA biplots of chironomids in the surface sediments of Lake Bolshoe Toko. (a) Common chironomid taxa
 483 and significant environmental variables. (b) Chironomid sampling sites and significant environmental variables.
 484



485
 486
 487
 488
 489

Fig. 4 Endmember analysis grain-size distributions in 33 samples from Lake Bolshoe Toko.



490
491
492
493
494

Fig. 5 Pearson correlation matrix of selected environmental parameters. Positive correlations indicated in red, negative correlations indicated in blue. A p values adjustment was applied and only values of <0.05 used to assign colours.

495 4 Results

496 4.1 Water chemistry

497 The sampled surface waters of Bolshoe Toko (Table 1) are well saturated in O₂
498 (101-113 %) with a pH-value in the neutral range (6.8 – 7.2). The electrical
499 conductivity is very low for all waters, though the lagoon shows a slightly higher
500 conductivity (67.8 $\mu\text{S/cm}$) than the rest of the samples (35.1 – 39.1 $\mu\text{S/cm}$). Traces
501 of Al (mean 72 $\mu\text{g/L}$), Fe (mean 46.6 $\mu\text{g/L}$), and Sr (mean 37.1 $\mu\text{g/L}$) were found.
502 However, there was no evidence for significant concentrations of environmental

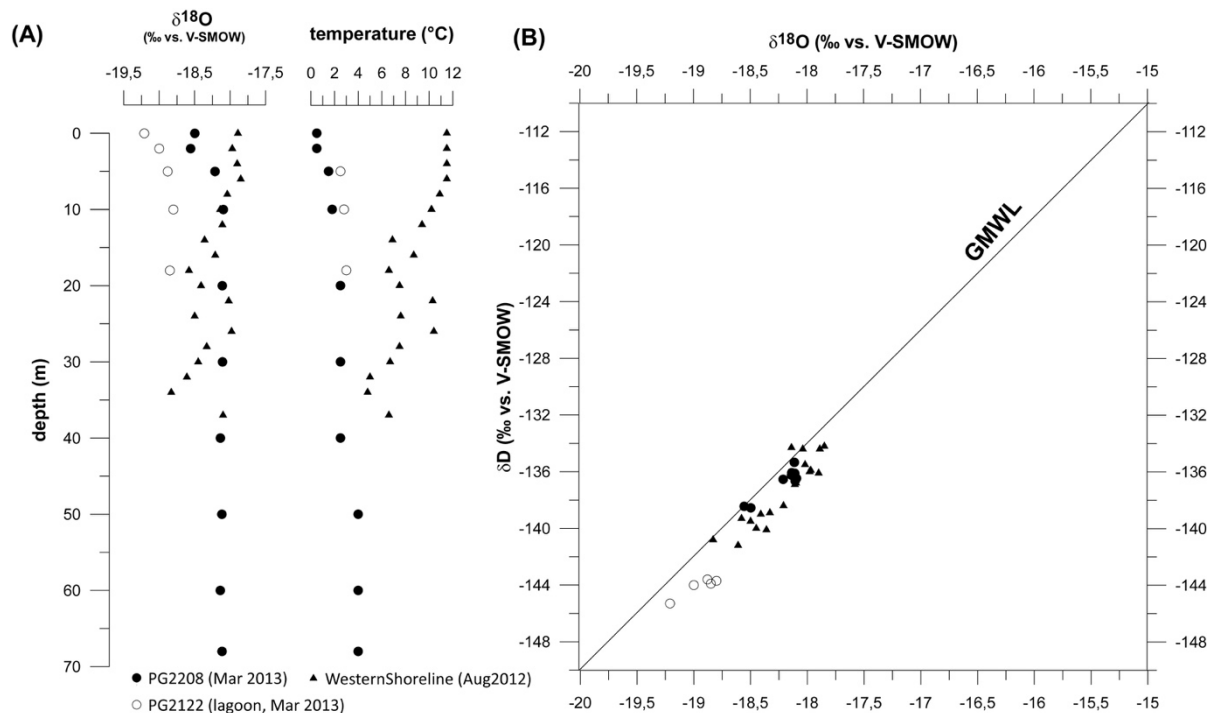
503 relevant elements (Pb, Cr, V, Co, Ni, Cu). The concentrations of sulfate (SO_4^{2-}) was
504 2.35 mg/l on average but lower in the lagoon (0.51 mg/l). The concentrations of
505 nitrate (NO_3^-) was 0.76 mg/l, but lower in the lagoon (0.29 mg/l). HCO_3^- was 37.52
506 mg/l in the lagoon and 14.9 mg/l on average in the rest of the samples. There was
507 no phosphorus found in any of the samples. Overall the water can be characterized
508 as water of the Ca-Mg- HCO_3 type.

509 The mean stable isotope composition of Bolshoe Toko lake surface waters at the
510 six coring positions is -18.7‰ for $\delta^{18}\text{O}$, -140.2‰ for δD and 9.5‰ for d-excess,
511 respectively. A relatively uniform isotopic composition of $\delta^{18}\text{O} = -18.58 \pm 0.15\text{‰}$ ($\delta\text{D} =$
512 $-139 \pm 0.7\text{‰}$) was observed for the main Bolshoe Toko waters, whereas the lagoon
513 (PG2122) displays slightly more negative $\delta^{18}\text{O}$ (δD) values of -19.2‰ (-145‰).
514 Water depth profiles were taken during the March 2013 expedition from the deepest
515 part of the lake (PG2108, water depth 70m) and in the lagoon (PG2122, 18m) as
516 well as in August 2012 (sample site near the western shoreline, 37m). The
517 temperature was determined in the field and the samples analysed for isotopes
518 ($\delta^{18}\text{O}$, δD , see Fig. 6). The mean isotopic composition of the water profile at PG2208
519 stabilizes from 10 m downward ($\delta^{18}\text{O} = -18.2 \pm 0.2 \text{‰}$) and is slightly heavier than
520 the surface samples ($\delta^{18}\text{O} = -18.6$) due to isotopic fractionation during ice formation.
521 In contrast, the lagoon shows a lighter isotope composition ($\delta^{18}\text{O} = -18.9 \pm 0.2 \text{‰}$)
522 than the main lake basin. Samples taken in August 2012 close to the western
523 shoreline show a similar mean value down the water column ($\delta^{18}\text{O} = -18.2 \pm 0.3 \text{‰}$)
524 but no change in the upper samples as seen in PG2208. A similar mean isotopic
525 composition indicates negligible evaporation effects and no strong seasonal change.
526 This is typical for through-flow lakes (Mayr et al., 2007). Generally, a higher variation
527 is observed in the August record. Meteorological data from the nearby weather
528 station (Toko RS, 10 km northward) recorded heavy rainfall for August 2012 (25 mm
529 above the long term mean of 83 mm). Such precipitation events could cause
530 temporary isotopic stratification or a variation in the isotopic signal throughout the
531 water column. Due to ongoing mixing, these variations are then evened. In
532 conclusion, variations in the isotopic composition throughout the August profile are
533 more a temporal phenomenon and not characteristic for Bolshoe Toko. All samples
534 are positioned close to the global mean water level (GMWL, Fig. 6) indicating an
535 unaltered precipitation signal without significant evaporation.

536
537
538
539
540
541
542

Table 1: Hydrochemical parameters from surface water samples of Lake Bolshoe Toko.

| | Unit | PG2207 | PG2208 | PG2122* | PG2124 | PG2125 | PG2126 | Average |
|-------------------------------|------------------|--------|--------|---------|--------|--------|--------|----------------|
| pH | | 6.95 | 6.81 | 6.99 | 7.05 | 7.24 | 7.13 | 7.03 |
| Conductivity | $\mu\text{S/cm}$ | 38.40 | 35.10 | 67.80 | 37.90 | 39.10 | 36.60 | 42.48 |
| Oxygen | % | 100.9 | 110.9 | 108.4 | 110.4 | 108.9 | 113.1 | 108.8 |
| Al | $\mu\text{g/L}$ | 82.18 | 79.88 | 43.19 | 75.54 | 73.31 | 77.62 | 71.95 |
| Ba | $\mu\text{g/L}$ | < 20 | < 20 | < 20 | < 20 | < 20 | < 20 | < 20 |
| Ca | mg/L | 5.00 | 4.73 | 9.01 | 4.68 | 4.91 | 4.70 | 5.51 |
| Fe | $\mu\text{g/L}$ | 24.56 | 26.90 | 147.56 | 24.96 | 33.13 | 22.22 | 46.55 |
| K | mg/L | 0.37 | 0.36 | 0.40 | 0.36 | 0.40 | 0.37 | 0.38 |
| Mg | mg/L | 1.16 | 1.09 | 2.71 | 1.07 | 1.13 | 1.10 | 1.38 |
| Mn | $\mu\text{g/L}$ | < 20 | < 20 | < 20 | < 20 | < 20 | < 20 | < 20 |
| Na | mg/L | 0.74 | 0.78 | 1.61 | 0.77 | 0.79 | 0.76 | 0.91 |
| P | mg/L | < 0,10 | < 0,10 | < 0,10 | < 0,10 | < 0,10 | < 0,10 | < 0,10 |
| Si | mg/L | 2.11 | 1.93 | 3.01 | 1.98 | 2.05 | 2.05 | 2.19 |
| Sr | $\mu\text{g/L}$ | 27.40 | 25.86 | 90.57 | 26.28 | 26.29 | 26.07 | 37.08 |
| Pb | $\mu\text{g/L}$ | < 25 | < 25 | < 25 | < 25 | < 25 | < 25 | < 25 |
| Cr | $\mu\text{g/L}$ | < 20 | < 20 | < 20 | < 20 | < 20 | < 20 | < 20 |
| V | $\mu\text{g/L}$ | < 20 | < 20 | < 20 | < 20 | < 20 | < 20 | < 20 |
| Co | $\mu\text{g/L}$ | < 20 | < 20 | < 20 | < 20 | < 20 | < 20 | < 20 |
| Ni | $\mu\text{g/L}$ | < 20 | < 20 | < 20 | < 20 | < 20 | < 20 | < 20 |
| Cu | $\mu\text{g/L}$ | < 20 | < 20 | < 20 | < 20 | < 20 | < 20 | < 20 |
| Zn | $\mu\text{g/L}$ | < 20 | < 20 | < 20 | < 20 | < 20 | < 20 | < 20 |
| Fluoride | mg/l | < 0,05 | < 0,05 | < 0,05 | < 0,05 | < 0,05 | < 0,05 | < 0,05 |
| Chloride | mg/l | 0.51 | 0.51 | 0.55 | 0.60 | 0.60 | 0.58 | 0.56 |
| Sulfate | mg/l | 2.72 | 2.47 | 0.51 | 2.66 | 2.95 | 2.77 | 2.35 |
| Bromide | mg/l | < 0,10 | < 0,10 | < 0,10 | < 0,10 | < 0,10 | < 0,10 | < 0,10 |
| Nitrate | mg/l | 0.82 | 0.82 | 0.29 | 0.82 | 0.88 | 0.89 | 0.76 |
| Phosphate | mg/l | < 0,10 | < 0,10 | < 0,10 | < 0,10 | < 0,10 | < 0,10 | < 0,10 |
| HCO ₃ ⁻ | mg/l | 15.71 | 13.58 | 37.52 | 14.80 | 15.41 | 15.10 | 18.69 |
| $\delta^{18}\text{O}$ | ‰ VSMOW | -18.72 | -18.5 | -19.21 | -18.63 | -18.43 | -18.71 | -18.70 |
| δD | ‰ VSMOW | -140.2 | -138.5 | -145.3 | -139.4 | -138.2 | -139.3 | -140.15 |
| d-excess | ‰ VSMOW | 9.6 | 9.4 | 8.4 | 9.7 | 9.2 | 10.4 | 9.45 |



547
548
549
550
551

Fig. 6: (A) Profiles of water isotopes ($\delta^{18}\text{O}$) and temperature from different locations taken in August and March. (B) $\delta^{18}\text{O}$ - δD diagram for various water samples. GMWL is the Global Meteoric Water Line (black line),

552 4.2 Physicochemical sediment composition

553 The typical surficial lake bottom sediments consist of either brown organic-
554 enriched gyttja or sandy, organic-poor siliciclastic material. Sand contents ranged
555 between 10.2 % and 96.2 % (mean 45.9 %, Fig. 7); silt contents ranged from 3.6 %
556 to 83.3 % (mean 47.1 %); clay contents ranged from 0.2 % to 11.3 % (mean 5.8 %).
557 Gravel was found only in four samples at the north eastern near-shore areas with
558 contents of up to 13.1 %. The mean grain size ranged from 12 to 479 μm (mean 72
559 μm). The mean grain size generally correlated negatively with water depth (r -0.45).
560 Mineral grains are composed mainly of quartz (32.7-76.2 %, mean 55.4 %),
561 plagioclase (13.4-39.5 %, mean 26.2 %), K-feldspar (0.0-9.8 %, mean 5.6 %), and,
562 to a smaller degree of pyrite (0.2-5.5 %, mean 3.3 %), hornblende (0.5-10.8 %,
563 mean 3.1 %), mica (0.3-2.4 %, mean 1.1 %), and the clay minerals smectite,
564 kaolinite and chlorite (together 0.0-4.6 %, mean 2.0 %). The spatial distribution of
565 minerals (Fig. 7) revealed a generally decreasing gradient of minerals relative to
566 quartz starting from the Utuk river delta (proximal) towards the northern areas
567 (distal).

568 The CLR transformed XRF data (Fig. 8) revealed high proportions of Zr and
569 intermediate to high Ti near the Utuk river inflow and at the northern and eastern
570 shore proximal areas. Zr values are seen to decrease with increasing water depth

571 towards the lake centre with the exception of the shallow lagoon where low values
572 are observed. Mn values are highest in the lake centre and at the very deep site at
573 the western steep subaquatic slope, and intermediate at shallow areas close to the
574 shore. A minimum in Mn is seen in the lagoon. Fe tends to be highest in the
575 southern part of the lake basin, in the very shallow site in the north, and in the
576 lagoon. Br demonstrates an unclear distribution; however high values are found at 2
577 sites within the eastern lagoon that correspond to high TOC contents.

578 Additive log ratios (ALR) of Mn/Fe were variable with intermediate values found at
579 sites surrounding the Utuk river inflow and low values within the lagoon and at basin
580 central sites. High values were located at the deepest lake site as well as in the
581 shallow north eastern region. Both Sr/Rb and Zr/Rb ratios demonstrated significantly
582 high values directly in front of the Utuk river inflow that diminished with distance
583 towards the basin center. Both Sr/Rb and Zr/Rb possessed intermediate to high
584 values in the north eastern lake region and suppressed values within the lagoon.
585 Si/Ti ratio values showed a trend from low in the southern lake region and lagoon to
586 high in the northern lake region.

587 The contents of total organic carbon (TOC, Fig. 9) ranged from 0.1 % to 12.3 %
588 (mean 4.9 %). Highest values appeared in the eastern area, intermediate values in
589 the central parts, and lowest contents in the northern shallow water areas. The
590 difference between TOC and total carbon is within the error of the devices and
591 hence no inorganic carbon was detected. TOC contents and the TOC/TN ratios are
592 highest near the Utuk river inflow in the southern part of the lake, in the lagoon, and
593 in proximity to the eastern shoreline. $\delta^{13}\text{C}$ was exemplary measured in 15 samples
594 and revealed maximum values at the eastern shore (-25.7 ‰) and minimum values
595 everywhere else (-27.8 ‰).

596

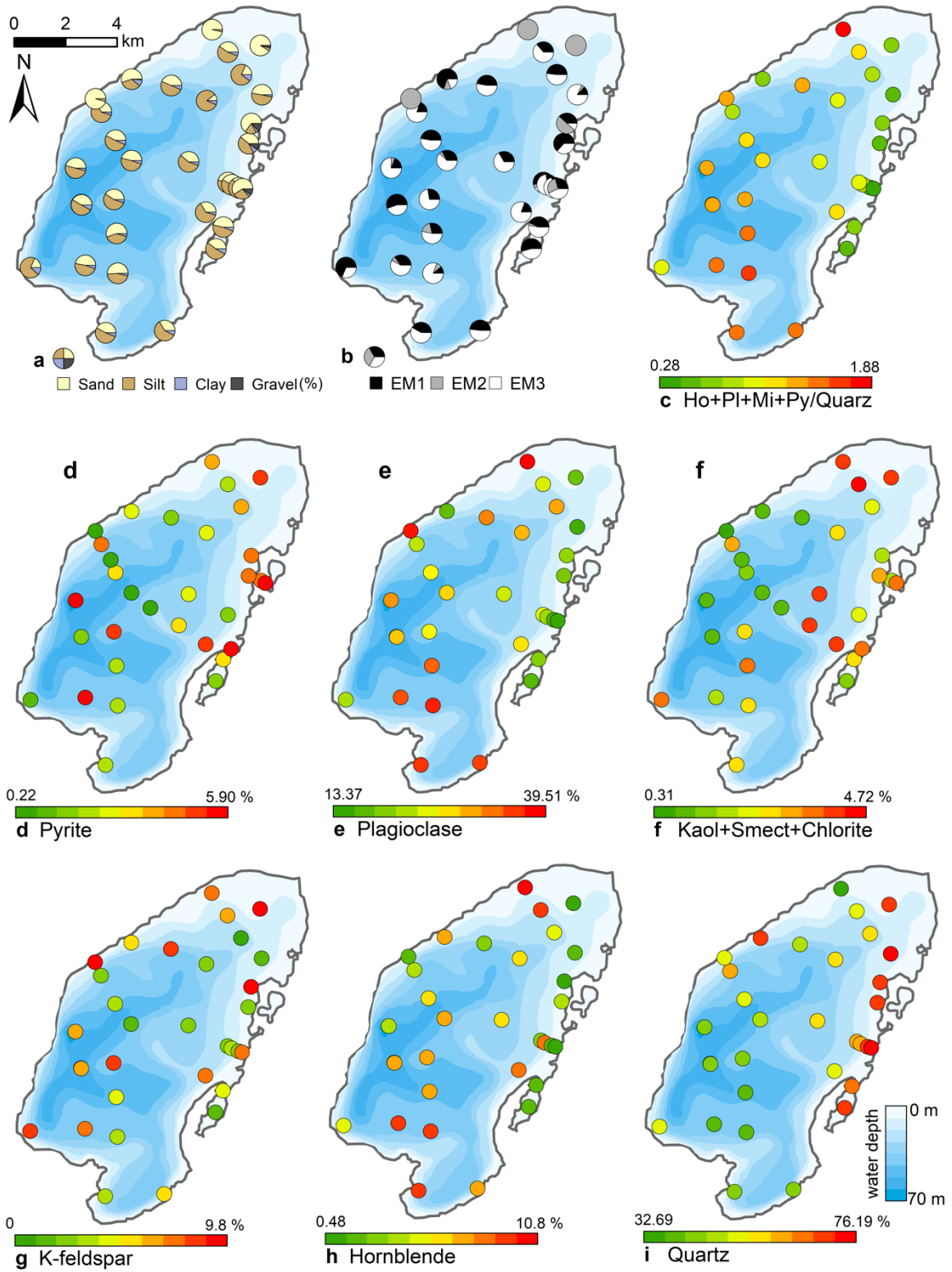
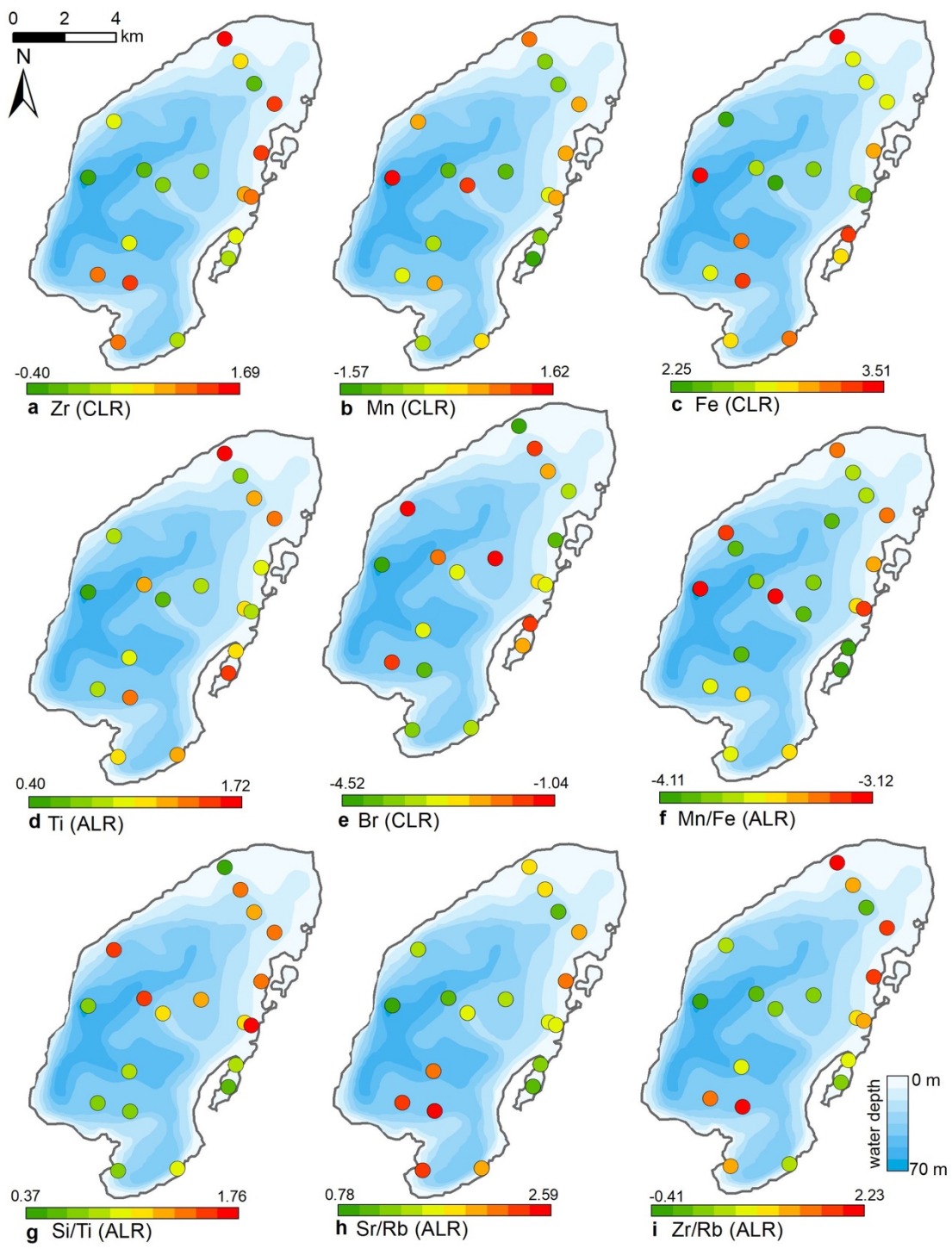


Fig. 7 Spatial distribution of the grain-size and mineral compositions of the surface sediments of Lake Bolshoe Toko.

597
598
599
600



601
 602
 603
 604

Fig. 8 Spatial distribution of elements obtained from XRF measurements of surface sediments of Lake Bolshoe Toko.

605 4.3 Diatoms

606 The diatom species assemblage in the analysed surface samples was generally
607 represented by boreal and arcto-alpine types and varied distinctly within Lake
608 Bolshoe Toko. In total, 142 diatom taxa were found in 23 sites, dominated by
609 planktonic species *Pliocaenicus bolshetokoensis* (Genkal et al., 2018) (0.0-27.9 %,
610 mean 14.7 %), *Cyclotella comensis* (0.0-23.1 %, mean 10.9 %), and benthic species
611 *Achnantheidium minutissimum* (0.0-38.0 %, mean 11.8 %). The relative content of
612 planktonic species (Fig. 9) was 2.0-73.7 % (mean 54.2 %), epiphytic species 19.2-
613 83.9 % (mean 36.4 %), and epibenthic species 2.6-23.0 % (mean 9.3 %). The
614 spatial distribution of the main taxa are shown in Fig. 10. Small benthic fragilarioid
615 species are represented by 0.0-27.6 % (mean 7.4 %), Naviculoid species ranged
616 from 3.3 % to 12.9 % (mean 7.2 %), and *Aulacoseira* species ranged from 0.0 % to
617 10.8 % (mean 4.5 %). *Pliocaenicus bolshetokoensis* maximal appearance was in
618 the areas with deepest water depth in the southern part of the lake and in the
619 eastern lagoon. *Cyclotella* species were more frequent in the central part of the lake
620 and were not as strictly bound to water depth as *Pliocaenicus*. *Aulacoseira* species
621 were distributed without clear patterns in the central part and less abundant in the
622 northern shallow water areas. *Tabellaria* species were more frequent in shallow
623 near-shore areas than in central and deep-water areas.

624 Achnanthoid (monoraphid) species were most abundant in near-shore areas,
625 especially near the eastern lake terrace. Fragilarioid (araphid) species were
626 common in the southernmost part near the inflow as well as in the lagoon. Other
627 benthic species, i.e. *Navicula*, *Cymbella*, and *Eunotia* were generally more abundant
628 in shallow near-shore areas than in deeper water areas.

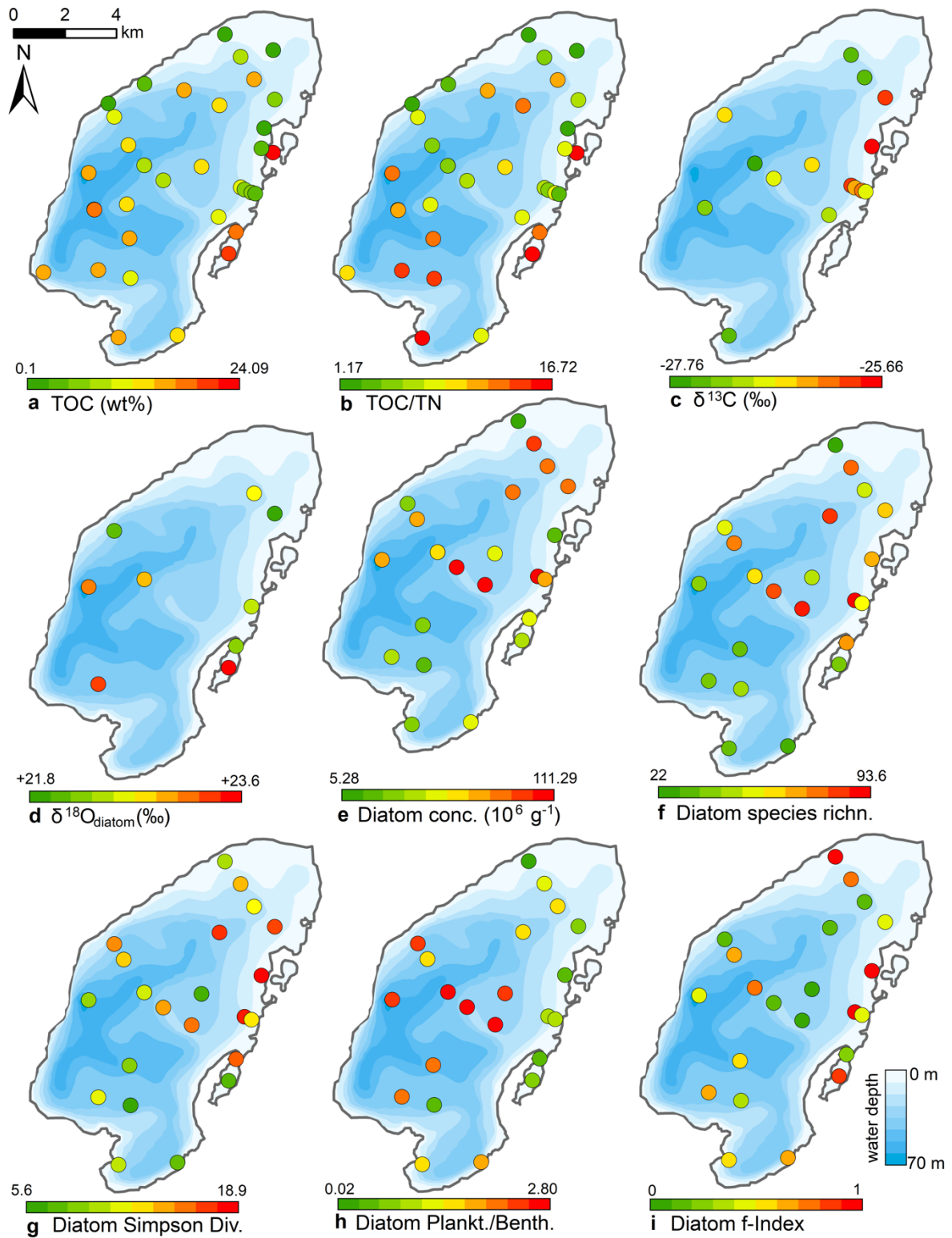
629 In pelagic areas planktonic diatoms were generally more abundant ~~principally in~~
630 ~~pelagic areas~~ than epiphytic and epibenthic species. Epiphytic species, however,
631 predominated in some shallow areas in the north and east parts of the lake.
632 Epibenthic species occurred in smaller abundancies in shallow lake littorals.
633 Together with an increased amount of non-planktonic species, the Simpson diatom
634 species diversity was higher in northern and eastern parts of the lake. The
635 chrysophytes index was higher near the river inflow in the south and along the river-
636 like bathymetrical structure and in the lagoon, where another small river runs into
637 the lake. **The Mallomonas index** was high near the inflow and in the central part, and
638 it was low at near-shore areas in the north and east. Highest f-index, representing
639 the best valve preservation, was found in the near shore areas, whereas lowest
640 values were found at a shallow bathymetrical structure in the central part of the lake.
641 The highest valve concentrations were observed in the central and northern lake
642 basin.

643 The initial RDA with all environmental variables showed that the axes 1 and 2
644 explained 39.6 % of variance of diatom species data. After deleting all

645 intercorrelated variables, 13 parameters with VIFs <20 were left for manual
646 selection with Monte-Carlo test. It revealed 8 statistically significant ($p \leq 0.05$)
647 explanatory variables: TOC/TN, TOC, water depth, distance from River, distance
648 from the shore, presence of vegetation, Sand, and EM3, (ESM diatoms, Fig. 2).
649 Eigenvalues for RDA axes 1 and 2 constrained by eight significant environmental
650 variables constitute 81% and 59%, respectively, of the initial RDA, suggesting that
651 the selected significant variables explain the major variance in the diatoms data.
652 The RDA biplots of the species scores and sample scores (Fig. 2) show that diatom
653 species and sites are grouped according to the main environmental forcing
654 responsible for their spatial distribution. The clearest environmental signals in the
655 RDA are related to water depth, habitat preferences and river influence. The upper
656 left quarter of the biplot is strongly influenced by water depth, grain size (EM3), and
657 the ratio between TOC and TN. The species found next to water depth are
658 planktonic *Cyclotella* taxa, whereas *Aulacoseira* is closer to TOC/TN and the total
659 carbon content. In the lower right quarter epiphytic and benthic taxa prevail, i.e.
660 achnanthoid, naviculoid and cymbelloid taxa, associated to the presence of
661 vegetation and coarser (sand) substrate conditions. The distances to river and to
662 shore are crossing the lower left quarter and are associated to different planktonic
663 *Cyclotella* and achnanthoid taxa, while in the opposite direction, with increasing
664 Utuk river influence, fragilarioid taxa, *Eunotia*, *Tabellaria*, and *Gomophonema*
665 prevail, next to the high influence of TOC/TN.

666 The $\delta^{18}\text{O}_{\text{diatom}}$ averages +22.8 ‰ (min. +21.9 ‰, max. +2.6 ‰, n=9, Fig. 9) with a
667 spatial distribution of higher values around 23.3 ‰ in the deeper south-western part
668 of lake (PG2113, 2115, 2005) where as low values of app. 22.3 ‰ prevail in the
669 shallower northern lake basin (PG2139, 2140, 2147, 2209). The two samples from
670 the lagoon show 22.2 ‰ in the shallower northern area and 23.6 ‰ in the deeper
671 part. Generally, the surface sediment $\delta^{18}\text{O}_{\text{diatom}}$ show a standard deviation of ± 0.6
672 ‰ (1σ). Four samples from the southern part could not be purified well enough and
673 show contamination corrections >2 ‰.

674



675
676
677
678

Fig. 9 Spatial distribution of organic properties and statistical parameters inferred from diatom assemblages in the surface sediments of Lake Bolshoe Toko.

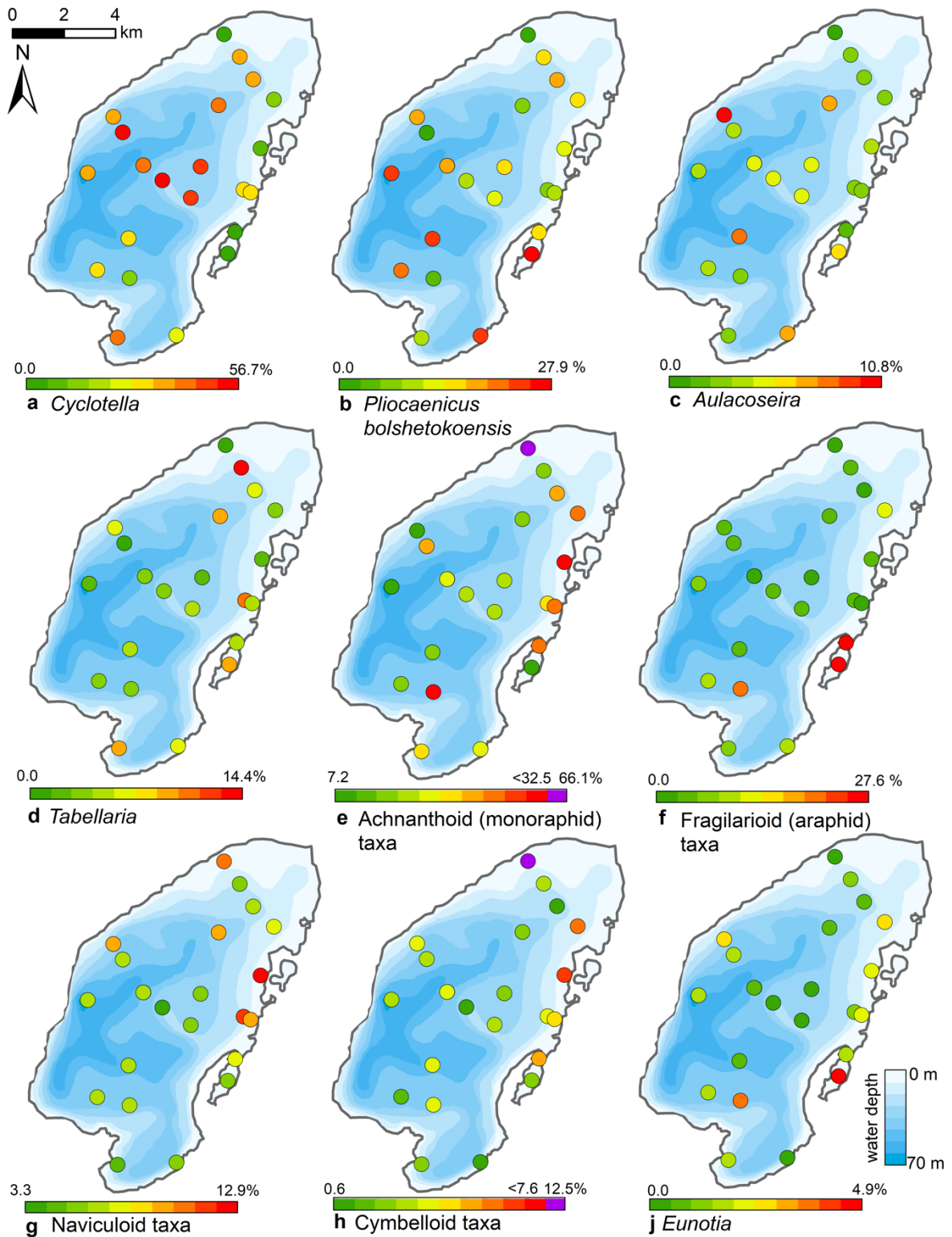


Fig. 10 Spatial distribution of main diatom taxa in the surface sediments of Lake Bolshoe Toko.

679
680
681

682 4.4 Chironomids

683 In the surface sediment samples, we identified in total 79 chironomid taxa of
684 which 48 belonged to subfamily Orthocladiinae, 25 to subfamily Chironominae (15
685 from the triba Tanitarsini and 10 from the triba Chironomini), 4 taxa were from
686 subfamily Diamesinae and 2 from Tanypodinae.

687 The initial RDA with all environmental variables shows that the RDA axes 1 and 2
688 explained 46.7% of variance in taxon data. Most of the environmental parameters
689 appeared to be intercorrelated and after deleting one by one all redundant variables,
690 eight parameters with VIFs <20 remained for the further analysis. The manual
691 selection with Monte-Carlo test selection revealed 4 statistically significant ($p \leq 0.05$)
692 explanatory variables: TOC/N, water depth (WD), distance from River, and presence
693 of vegetation (Table 2). Eigenvalues for RDA axes 1 and 2 constrained by four
694 significant environmental variables were 0.200 and 0.150, respectively. They
695 constitute 70 and 85 % of the RDA performed on all environmental variables (0.289
696 and 0.177, respectively). This minor difference suggests that the four selected
697 variables sufficiently explain the major gradients in the chironomid data.

698 The RDA biplot of the sample scores shows that sites are grouped by their
699 location in relation to the major environmental variables (Fig. 11) and distribution of
700 chironomid taxa along the RDA axes reflects their ecological spectra. Table 2 and
701 Fig. 11 show median values of eco-taxonomical chironomid groups and their relation
702 to environmental parameters.

703 Sites most strongly influenced by the inflowing rivers are grouped in the lower
704 left quarter of the biplot, as the vector in the upper right quarter shows an increase
705 of the distance from the river mouth. In total 64 chironomid taxa have been found in
706 this group of sites, and of these 33 have been found only here. Chironomid fauna is
707 represented by mainly phytophilic littoral taxa from the Orthocladiinae genera
708 *Cricotopus*, *Orthocladus*, *Eukiefferiella*, and *Parakiefferiella* etc. (Fig. 11). Another
709 important feature of the fauna here is the presence of a relatively high amount of the
710 taxa characteristic for lotic environments, among which are several *Diamesa* taxa,
711 *Rheocricotopus effusus*-type, *Synorthocladus*, *Brillia*, and for lotic-lentic
712 environments like *Parakiefferiella bathophila*-type, *P. trigueta*-type, *Nanocladus*
713 *rectinervis*-type, *N. branchicolus*-type, several *Eukiefferiella* taxa, and
714 *Stictochironomus*.

715 The group in the opposite upper right quarter represents the northern part of
716 the lake situated far from the inflowing rivers. Here, mainly profundal taxa prevail,
717 i.e. *Procladius*, *Polypedilum nubeculosum*-type, *Cryptochironomus* (eurytopic), and
718 *Heterotrissocladus maeaeri*-type 1 (acidophilic).

719 The lower right group of sites represent eastern shallow littoral with presence
720 of macrophytes. Species richness and proportion of semiterrestrial and littoral taxa
721 in this group is generally low. 29 chironomid taxa were found here and 5 taxa were

722 found only in this group of sites. Littoral taxa here are generally phytophilic:
 723 *Cricotopus intersectus*-type, *C. cylindraceus*-type, *Dicrotendipes nervosus*-type
 724 (mesotrophic), and *Cladotanytarsus mancus*-type and *Psectrocladius sordidellus*-
 725 type (acid-tolerant mesotrophic). Most abundant profundal taxa here belong to the
 726 acid-tolerant *Heterotrissocladius* genera represented by *H. macridus*-type, *H.*
 727 *maeaeri*-type 1 and 2, *H. grimschawi*-type (acidophilic), and to the subfamily
 728 Tanypodinae represented by *Procladius*. The sites grouped in the opposing upper
 729 left quarter represent lotic and lotic-lentic taxa (*Diamesinae*, *Thenimaniella*
 730 *clavicornis*-type, *Eukiefferiella claripennis*-type, *Eukiefferiella fittkaui*-type, several
 731 *Orthocladius* taxa).

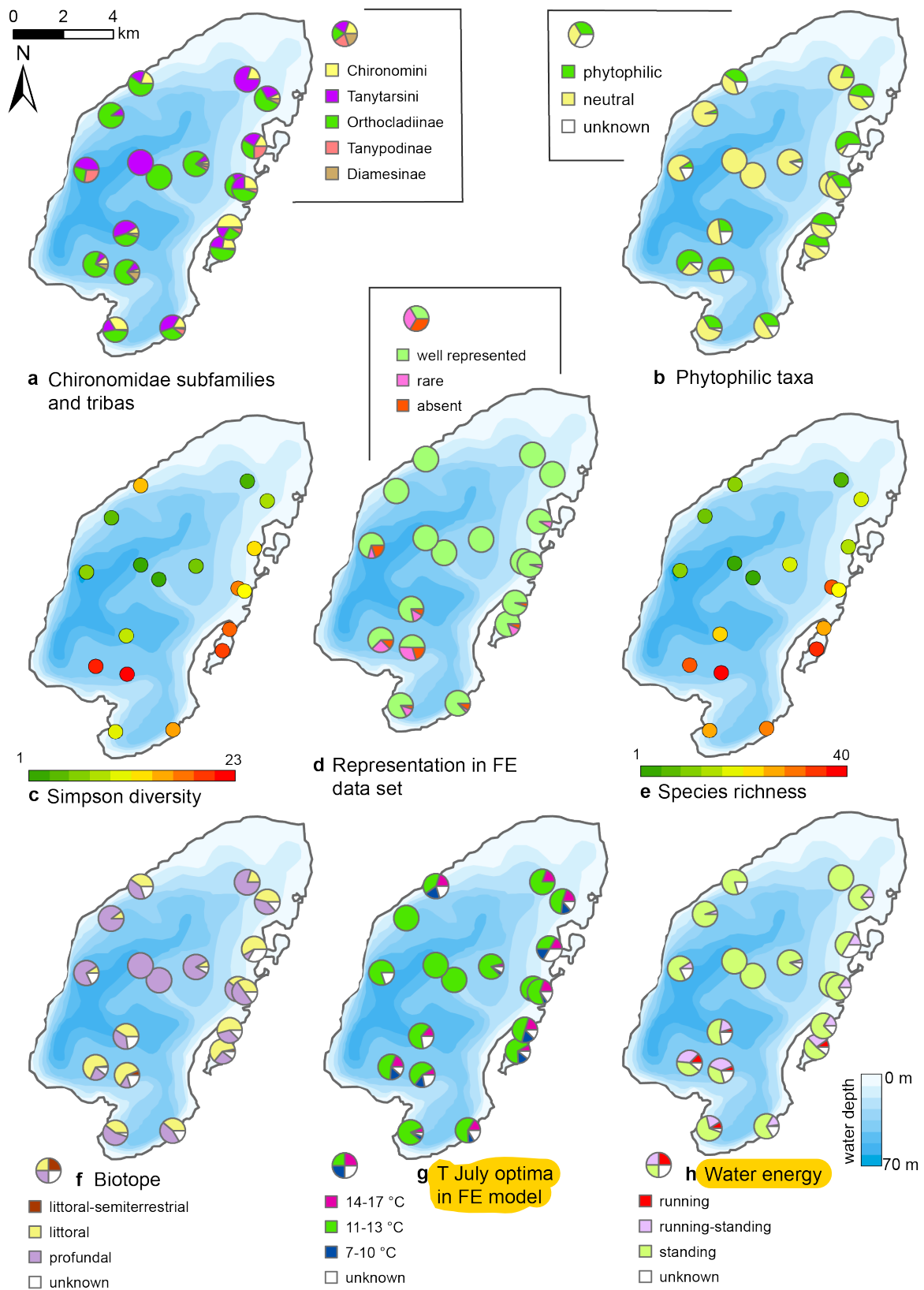
732
733

734 **Table 2.** Median representation of ecological chironomid groups in the modern FE chironomid based
 735 training set (Nazarova et al., 2015) in relation to mean July temperature, biotopes, water velocity, and
 736 presence of macrophytes (vegetation) in groups of sites revealed by the RDA. UN- unknown (all
 737 specimens that were identified to subfamily level only due to bad heads preservation or no
 738 information available); ST – semiterrestrial; L - littoral; P – profundal; R – river (lotic); S – standing
 739 water (lentic); F – phytophilic; N – neutral.

740

| Group of sites | T optima, °C | | | | Biotope | | | | Water velocity | | | | Vegetation | | | Representation in the modern FE training set |
|----------------|--------------|-------|-------|-------|---------|-------|-------|-------|----------------|-------|-------|-------|------------|-------|-------|--|
| | 14-17 | 11-13 | 7-10 | UN | L-ST | L | P | UN | R | R-S | S | UN | F | N | UN | |
| River | 8.51 | 53.57 | 13.83 | 12.50 | 1.79 | 59.83 | 32.34 | 10.71 | 8.64 | 27.66 | 52.13 | 10.71 | 46.25 | 41.25 | 10.71 | 80.78 |
| Eu Littoral | 16.50 | 57.43 | 12.33 | 16.93 | 0.00 | 38.98 | 36.31 | 16.93 | 0.00 | 14.64 | 68.67 | 16.93 | 34.85 | 49.49 | 16.93 | 91.69 |
| Sub Littoral | 12.08 | 81.67 | 2.08 | 4.17 | 0.00 | 15.00 | 59.58 | 4.17 | 0.00 | 2.08 | 91.25 | 4.17 | 12.50 | 83.75 | 4.17 | 100 |
| Profundal | 0.00 | 72.73 | 0.00 | 22.73 | 0.00 | 9.09 | 50 | 18.18 | 0.00 | 9.09 | 72.73 | 18.18 | 9.09 | 72.73 | 18.18 | 78.03 |

741
742



743
744
745
746

Fig. 11 Spatial distribution of chironomid taxa and inferred statistical parameters in the surface sediments of Lake Bolshoe Toko.

747 5 Discussion

748 5.1 Spatial control of abiotic and biogeochemical sediment 749 components

750 Physical properties of particles within the surface sediments of Bolshoe Toko
751 depend chiefly on transportation processes and the characteristics and availability of
752 clastic compounds in the source areas in the lake catchment. The main catchment
753 comprises the Stanovoy mountain range in the south channelled through the Utuk
754 river into Bolshoe Toko. Accordingly, the lake experiences annual input of
755 suspended material through a single source at the Utuk river mouth that likely is at
756 its maximum during spring snow melt (Bouchard et al., 2013). The grain-size data
757 and its end-members (Fig. 4 and 7) show that the proportions of sand, silt, and clay
758 remain somewhat constant in proximity to the Utuk river inflow but change towards
759 the north and at the lake shoreline. Whereas in the central northern lake basin the
760 amount of silt increases, the proportions of sand increase along the northern
761 shoreline on top of the drowned moraine. Gravel is only present in samples near the
762 lake terraces in the east. The constant distribution in the south-central lake basin
763 reflects the river input. Decreasing river influence and hence decreasing water
764 transport energy with increasing distance from the river mouth leads to the observed
765 predominance of finer grain-sizes (silt dominated) samples in the northern central
766 parts of the lake. Sandy samples along the shoreline reflect direct input from the
767 moraines around the northern part of the lake. Other relevant within-lake
768 sedimentary processes include shore-erosion and inwash and winnowing of fine
769 sediment grains by surface currents as well as alluvial processes and debris flows
770 which continue basin ward as subaquatic flows. The restriction of gravel at the
771 eastern shore can be attributed to the availability of source material and suitable
772 transport pathways of coarser clasts from the third moraine. In consequence to the
773 described lateral transport trajectories and local control factors within the lake, there
774 is only weak negative correlation between mean grain size and water depth ($r -0.45$,
775 Fig. 7 and 12).

776 The modelled end-member loadings of the observed grain-size classes (Fig. 4 and
777 7) indicate EM1 having the major peak in fine silt representing mainly fluvial
778 sediment input. EM2 having its peak values in fine to medium sandy grain-size
779 fractions and in the northern part of the lake points to depositional processes
780 associated with the erosion of moraines distal from the river inflow, where the
781 hydrological dynamics in the lake basin are weak. As shown by a weak positive
782 correlation between EM3 and the concentration of diatom valves ($r 0.44$), EM3 likely
783 represents both in-situ diatom valves, that could not be removed from the
784 allochthonous sediment particles during our sample processing, and possibly ice-
785 rafted debris that is transported over the lake after ice break up (Wang et al., 2015).

786 Intermediate concentration of TOC and high ratios of TOC/TN in the south as
787 compared to the north suggest differences in catchment characteristics, i.e. a
788 considerable allochthonous contribution of terrestrial plant material from the Utuk
789 river. This assumption is supported by previous findings that showed that non-
790 vascular plants, i.e. phytoplankton and other algae, usually have TOC/TN ratios
791 between ca. 5 and 10 while organic matter from vascular land plants has higher
792 values of about 20 (Meyers and Teranes, 2002). High values of TOC/TN in lake
793 sediment surfaces at river inflows have also been observed in other studies (Vogel
794 et al., 2010). $\delta^{13}\text{C}$ was generally low on average (-26.8) and only slightly higher at
795 the eastern shore (-25.7), suggesting a strong overall dominance of C_3 plants and
796 phytoplankton in the bulk organic matter fraction (Meyers, 2003). It is yet unclear to
797 what degree old and reworked organic carbon, e.g. from charcoal deposits, is
798 transported to the lake.

799 The distribution of elements from the XRF scanning data suggests strong abiotic
800 relationships to grain-size and mineral distributions. We focus on heavier elements
801 because lighter elements, even though they are commonly present in higher
802 concentrations, show potential contribution from multiple sources. Sr/Rb ratios and
803 Zr are negatively correlated with Kaolinite/Chlorite (r -0.73 and -0.85, respectively).
804 As described in Kalugin et al. (2007), Rb substitutes for K in clay minerals. The
805 Sr/Rb ratios do not show however a significant correlation with grain-size
806 parameters as found in other studies (Biskaborn et al., 2013b). We assume
807 therefore that Sr, as substituent for Ca, is influenced by multiple minerals
808 represented in different grain-size fractions, i.e. K-feldspar (r 0.45) and Hornblende
809 (r 0.24). Associated to high metamorphic grades in the Stanovoy mountains, Sr is
810 preferentially taken into the K-feldspar phase (Virgo, 1968). The Zr/Rb ratio on the
811 other hand, correlates well with the sand fraction (r 0.50) and with the mean grain
812 size (r 0.49), but negatively with silt (r -0.54) and clay (r -0.39). We explain this effect
813 by a higher diversity of minerals caused by the input of the Utuk river supplying the
814 lake basin with mafic Ca-rich metamorphic rocks from the Stanovoy mountains. The
815 strong influence of the Utuk river in the spatial distribution of physicochemical
816 sediment components is demonstrated by the decreasing gradient of minerals
817 relative to quartz starting from the Utuk river towards the northern lake basin (Fig.
818 7). The most representative indicator of grain size variations in surface sediments is
819 given by clr transformed values of Ti which correlate well with the sand fraction (r
820 0.74) and the mean grain size (r 0.88).

821 Si/Ti ratios have been used previously as a proxy for the biogenic silica content of
822 sediments (Melles et al., 2012). This stems from the fact that Ti is generally
823 attributed to detrital influx and Si to both detrital and biogenic (diatom) origins. At
824 Bolshoe Toko somewhat positive correlations between Si/Ti ratios, diatom valve
825 concentrations (r 0.36) and the ratio of planktonic to benthic diatoms (r 0.42)

826 suggests that Si/Ti may be useful to trace the relative portion of diatom valves in
827 intermediate grain-size fractions. Moreover, the Si/Ti ratio correlates significantly
828 with silt (r 0.81).

829 Mn/Fe ratios have often been ascribed to redox dynamics associated to bottom
830 water oxygenation processes (Naehler et al., 2013). In Bolshoe Toko, however, the
831 detrital input of ferrous minerals, i.e. pyrite, suggests that the Mn/Fe ratios cannot
832 directly be used effectively to track redox processes in the surface sediments. This
833 is supported by the correlation of Fe with the sand fraction (r 0.6) and grain-size (r
834 0.59). Accordingly, we found no significant correlations between Mn/Fe and other
835 abiotic or biotic proxies.

836 There is an uncertainty in the spatial distribution of elements measured by XRF
837 techniques. We attribute this lack of clear patterns to two main reasons: (1)
838 methodological hurdles to apply XRF techniques to surface sediments commonly
839 rich in water and organic material, and (2) multiple sources of the same elements
840 coming from minerogenic input, grain-size differences in individual samples and
841 different intensities of redox processes at different habitat settings. The high
842 variance of elements therefore should be seen as a representation of the high
843 complexity of this lake system rather than unequivocal validations or falsifications of
844 the applicability of XRF scanner data as an environmental proxy at Bolshoe Toko.

845

846

847 **5.2 Factors explaining the spatial diatom distribution**

848 Given the fact that diatoms react rapidly to environmental changes, different
849 driving factors influence the diatom distribution at different sites including
850 hydrochemical parameters, water depth, nutrients, and catchment vegetation type
851 (Pestryakova et al., 2018). Planktonic diatom species have appeared to have
852 spread over the entire Lake Bolshoe Toko, with a distinct tendency of the ratio
853 between planktonic and benthic species to greater water depths (r 0.74, Fig. 5 and
854 12), due to the limited availability of light for benthic species, as reported in other
855 lakes (Gushulak et al., 2017; Raposeiro et al., 2018). Especially *Aulacoseira* species
856 were never abundant along the shallower northern and eastern shorelines. The
857 main difference between the two most abundant genera in the lake was that
858 *Pliocaenicus* showed highest abundancies in proximity to the inflow and in the
859 southeastern lagoon, whereas *Cyclotella* valves were more frequent in the lake
860 center and absent in the lagoon. There is yet little known about the new species
861 *Pliocaenicus bolshetokoensis* (Genkal et al., 2018). Our findings suggest factors
862 other than water depth (r 0.39), such as proximity (e.g. nutrient supply) to the Utuk
863 river and small streams, as controlling parameters for bloom intensities of this
864 species. *Cyclotella*, however, is restricted to stratification of the water column and

865 hence is more abundant at distance from the river mouth, where incoming water
866 causes turbulence (Rühland et al., 2003; Smol et al., 2005). *Cyclotella* is therefore
867 also believed to benefit from recent air temperature warming trends and will likely
868 increase in abundance (Paul et al., 2010). *Aulacoseira* is a heavier, rapidly-sinking
869 tychoplanktonic group of species requiring water turbulence to remain in the photic
870 zone (Rühland et al., 2008; Rühland et al., 2015), which explains the lower
871 abundancies in the northern and quitter zones within the lake. *Tabellaria* species are
872 known to occur in a planktonic lifestyle with the help of zigzag colonies and relatively
873 lightly silicified frustules. However, they also can appear as short-valved
874 populations, which are believed to represent benthic forms (Lange-Bertalot et al.,
875 2011; Biskaborn et al., 2013a; Krammer and Lange-Bertalot, 1986-1991). In our
876 study, the spatial within-lake distribution of *Tabellaria* forms in Bolshoe Toko
877 indicates benthic habitats rather than planktonic lifestyle.

878 The most common non-planktonic species in Bolshoe Toko belong to
879 achnanthoid (monoraphid) genera, of which most species are epiphytic. Epiphytic
880 species showed a stronger negative correlation to water depth ($r = -0.68$), than
881 epibenthic species ($r = -0.4$), indicating that water plants, controlled by water
882 transparency, pH, water depth and nutrient status (Valiranta et al., 2011), represent
883 an important function in the lake ecosystem (Fig. 12). The highest amount of
884 achnanthoid and cymbelloid valves was found in at 400 m distance to the northern
885 shore at a water depth of 0.5 m.

886 Fragilarioid species are adapted to rapidly changing environments and thus
887 higher ecosystem variability (Wischnewski et al., 2011). The peak occurrences of
888 *Staurosira* species, which are pioneering small benthic fragilarioids (Biskaborn et al.,
889 2012), therefore indicates the formation of a new ecosystem habitat type in the
890 lagoon at the south-eastern lake basin. We assume that this basin is successively
891 being separated from the main basin and eventually will form a separated small
892 remnant lake following the example of the small “Banya” lake four kilometres from
893 the lagoon towards northeast (Fig. 1). High productivity of epiphytic species and low
894 detrital input suggested by elemental and grain-size data, together with higher
895 organic contents (High TOC and Br), indicate a calm sedimentological regime with
896 high bioproductivity. Similar neutral pH values measured in water samples from the
897 central basin and the lagoon (Table 1) questions pH as a main driving factor of the
898 *Eunotia* peak in the lagoon. However, Barinova et al. (2011) suggest 5.0-5.8 pH
899 range for the identified *Eunotia* species, which rather indicates that the pH values
900 obtained during April in 2013 are not representative for the annual average and the
901 specific catchment of the lagoon, which likely will differ from this point measurement.
902 The ice break-up during spring and transport of water from the catchment restricted
903 to the lagoon likely leads to milieu differences in the lagoon relative to the main
904 basin.

905 The RDA biplot of diatoms (Fig. 2) suggests that both, water depth and distance
906 to river are important lake attributes that explain the species distributions across the
907 lake. Especially *Eunotia*, fragilarioids, *Tabellaria*, and also *Aulacoseira subarctica*
908 appear more frequently at sites that are close to the Utuk river mouth (e.g. PG2113,
909 PG2115, PG2117, PG2118). The high TOC/TN ratios in these samples illustrates
910 the strong riverine input of allochthonous material. In the biplots, high water depth is
911 primarily associated to *Cyclotella* species (and *Aulacoseria*), while *Aulacoseira*
912 species tend to be additionally influenced by incoming rivers and also thrive closer
913 to the shorelines. Areas close to river mouths are usually dominated by river taxa
914 and species that prefer higher nutrient contents related to river input and associated
915 early ice cover melting (Kienel and Kumke, 2002). Accordingly, the influx of diatoms
916 from wetlands in the lake catchment is an important additional factor influencing the
917 spatial diatom distribution (Earle et al., 1988). As compared to conductivity, water
918 depth and nutrients, analyses on the direct relationship between temperature and
919 diatom species is poorly understood in Yakutian lake systems (Pestryakova et al.,
920 2018) and should be omitted.

921 Our RDA also shows that a high diversity of benthic, and especially epiphytic
922 diatom species, i.e. several achnanthoid species and some naviculoid taxa plot in
923 the opposite direction from water depth together with vegetation and the coarse
924 grain-size fraction. Kingston et al. (1983), revealed spatial diatom variability in the
925 Laurentian Great Lakes, where the stability of diatom assemblages increased with
926 water depth. In shallower marginal waters of the Great Lakes, the availability of
927 diverse habitats, including benthic and periphytic niches, leads to high species
928 diversity. According to our data in Bolshoe Toko, the Simpson index suggests higher
929 beta-diversities associated to increased habitat complexity (Kovalenko et al., 2012),
930 i.e. availability of water plants and benthic substrates in shallower depths along the
931 eastern and northern shore. The higher productivity in this area can be explained by
932 differential catchment preferences. However, it can be assumed that due to lesser
933 water supply rates from the small northern part of the catchment (Fig. 1), a single
934 spot at the north eastern lake margin will likely not receive significantly higher
935 loadings of nutrients as compared to the Utuk river coming from the igneous
936 mountain range. Nevertheless, moraine deposits typically contain high amounts of
937 silt and clay which can more easily be weathered and altered to fertilizing
938 substances that are transported into the calm and shallower northern part of the
939 basin.

940 The indices of crysophyte cysts and *Mallomonas* relative to diatom cells exhibited
941 indistinct patterns in the spatial distribution but a slight tendency towards high water
942 depths. Although crysophyte cysts commonly represent planktonic algae (Smol,
943 1988a), periphytic taxa are also common in boreal regions (Douglas and Smol,

944 1995) with cool and oligotrophic conditions (Gavin et al., 2011). *Mallomonas* was
945 reported as an indicator of lake eutrophication and acidification (Smol et al., 1984).

946 Taphonomic effects on the preservation of subfossil assemblages are generally
947 influenced by clastic transport mechanisms depending on the lake morphology
948 (Raposeiro et al., 2018). The preservation of diatom valves in Bolshoe Toko was
949 lowest in samples from a plateau-like feature at the central part of the lake bottom,
950 which indicates increased re-working associated to bottom currents and/or
951 increased dissolution of diatom valves due to lesser accumulation rates, and/or
952 increased grazing activity of herbivorous organisms (Flower and Ryves, 2009; Ryves
953 et al., 2001).

954 The spatial distribution of $\delta^{18}\text{O}_{\text{diatom}}$ from the sediment surface showed higher
955 $\delta^{18}\text{O}_{\text{diatom}}$ values at the deeper, south-western part of the lake with a difference of
956 app. 1‰ compared to lower $\delta^{18}\text{O}_{\text{diatom}}$ values in the shallower northern part. This
957 could be due to $\delta^{18}\text{O}_{\text{water}}$ variations, a difference in the average water temperature or
958 a varying species composition assuming a species-effect exists. Several studies
959 gave evidence that a species effect does not exist for this proxy (Bailey et al., 2014).
960 Additionally, the sieving step reduces the assemblage before the isotope analysis to
961 only a small size interval resulting in a similar species-composition. Regarding
962 variations in the isotope composition of the lake water surface waters sampled at
963 the same time in different parts of the lake show a very uniform isotopic composition
964 (within $\pm 0.15\text{‰}$) suggesting a well-mixed lake system and no strong seasonal
965 intermittency. As this is a one-time recording, slight seasonal variation between
966 shallower and deeper parts (for example due to evaporation) cannot be completely
967 excluded and could account for part of the differences in ^{18}O . An evaporation driven
968 heavier water isotope composition in the shallower parts would however result in
969 higher $\delta^{18}\text{O}_{\text{diatom}}$ values.

970 The lake temperature in which the diatoms grow has an impact of ca. $-0.2\text{‰}/^{\circ}\text{C}$
971 on the oxygen isotope signal (Brandriss et al., 1998; Dodd et al., 2012; Moschen et
972 al., 2005). Shallower areas heat up faster especially in the photic zone. The
973 temperature profile near to the western shoreline taken in August 2012 (Fig. 6)
974 shows 12°C at the surface with an average of app. 10°C in the first 15m of the water
975 column decreasing to app. 6°C in 30m depth. Although a spatial difference of 5°C in
976 the photic zone for causing a 1‰ shift is rather unlikely, this could account for part
977 of the variation in surface $\delta^{18}\text{O}_{\text{diatom}}$.

978
979

980 5.3 Factors explaining the spatial chironomid distribution

981 The RDA performed on chironomid data suggested that the most important factor
982 driving the spatial distribution of chironomids in the Bolshoe Toko was influence of

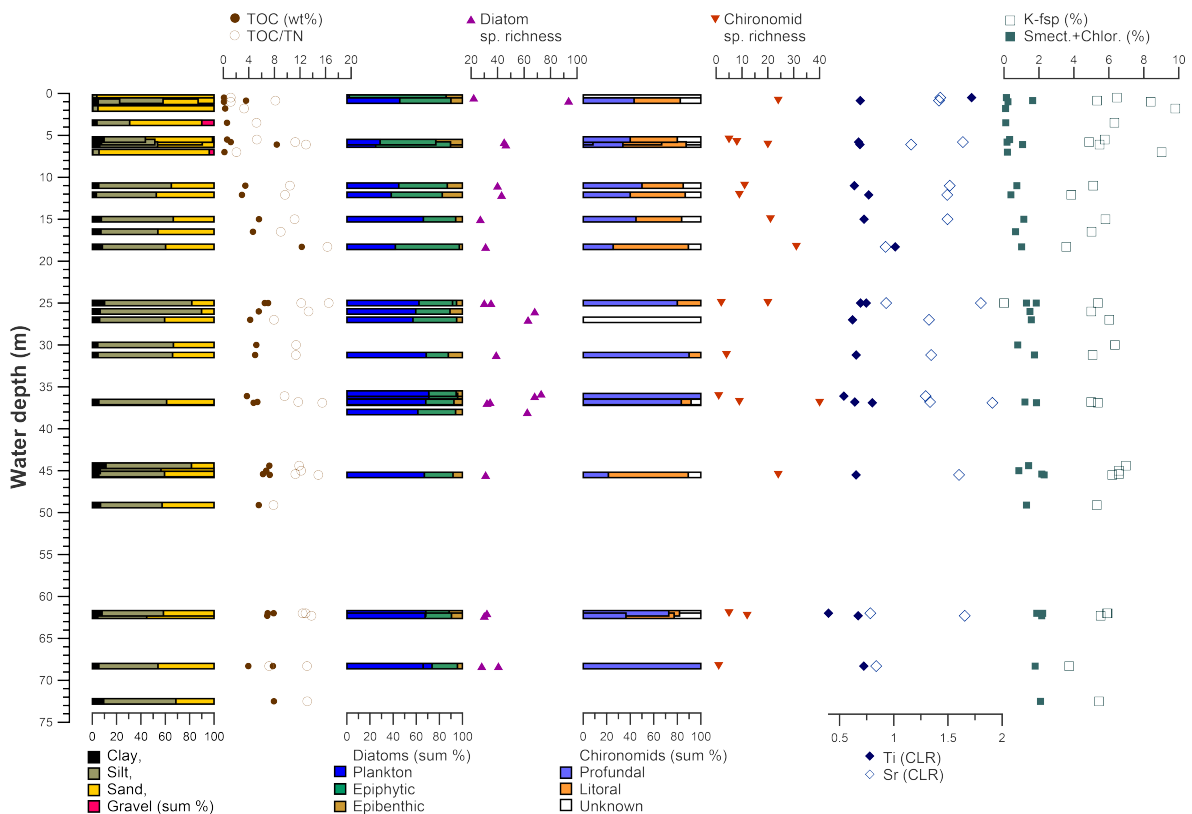
983 the tributary rivers. Influenced sites demonstrate high species richness with the
984 highest diversity being found at the site 2117 situated just opposite of the Utuk river
985 inflow and at the site PG2122, that is situated in the SE lagoon that gets water from
986 a small inflowing stream. Semiterrestrial taxa, like *Smittia-Parasmittia*,
987 *Pseudosmittia*, *Limnophies-Paralimnophies*, have been found only here with the
988 highest abundancies of 6 and 3.2% at the sites opposite of the inflowing rivers
989 (PG2117 and PG2122) suggesting that those taxa were transported from the dump
990 or marshy river deltas.

991 Species at lentic sites with no tributary influence were mainly controlled by water
992 depth. Deep profundal sites of the lake have much lower taxonomic richness of
993 chironomid communities. Higher taxonomic richness at site PG2118 can be
994 explained by an enriching riverine influence. High proportions of lotic and lotic-lentic
995 taxa lead to a high taxonomic similarity of this profundal site to littoral sites in the S
996 and SE. Similarly, in relation to temperature, sublittoral and profundal sites both
997 have much higher representation of the taxa characteristic of semi-warm conditions
998 and lower abundancies of the taxa preferring warm and cold conditions. However,
999 high depths of the sublittoral and profundal sites lead to the development of a poor
1000 chironomid fauna at these sites. High distance from the shore and presumably only
1001 weak transportation of chironomid remains of littoral fauna to the profundal zone
1002 could be another limiting factor for diversity of chironomid communities in the
1003 profundal.

1004 Eastern relatively shallow littorals are inhabited by more diverse, phytophilic,
1005 mesotrophic and partly acidophilic fauna with absence of lotic taxa, related to a less
1006 disturbed and turbulent environments and presence of macrophytes. This fauna has
1007 higher abundance of the semi-warm and warm taxa. The presence of meso- to
1008 eutrophic and acidophilic taxa can be attributed to paludification of the shore zone
1009 and decomposition of macrophytes and submerged vegetation in the shallow littoral
1010 (Nazarova et al., 2017b).

1011 It is still debated how spatial and local environmental processes influence the
1012 distribution of chironomids at a small spatial scale in a lake (Luoto and Ojala,
1013 2018; Yang et al., 2017). It is known that even within one water body the
1014 concentration of chironomid head capsules may vary from zero to several thousand
1015 per 1 cm³ of sediments (Kalinkina and Belkina, 2018; Walker et al., 1997),
1016 depending on the various ecological factors including the water depth, rate of
1017 sediment accumulation, the hydrological conditions, or anthropogenic influence.
1018 Water depth is a major driving factor of chironomid assemblages in many studies
1019 (Ali et al., 2002; Luoto, 2012; Vemeaux and Aleya, 1998) and depth optima of several
1020 species prove to be consequent across broad spatial scales (Nazarova et al., 2011).
1021 Taphonomy assumes that the assemblage of chironomid remains from the deepest
1022 zones of lake represents an assemblage of elements of profundal necrocenosis
1023 (Hofmann, 1971) mixed with secondary components of littoral fauna transported

1024 with in-lake hydrological and sedimentary processes into the profundal from outside.
 1025 Profundal necrocenosis therefore are supposed to include the assemblage of
 1026 remains of organism that inhabited the whole lake and are therefore the most
 1027 reliable indicators of ecological conditions in palaeoecological research (Brooks et
 1028 al., 2007).
 1029 The redeposition of littoral taxa into the profundal zone is an important factor that
 1030 affects the final composition and abundance of fossil assemblages and thus further
 1031 ecological information that can be derived from the assemblage. In small lakes,
 1032 fossil assemblages from the profundal zone quite adequately reflect the fauna of the
 1033 entire water body (Brooks and Birks, 2001; Walker and Mathewes, 1990). Our
 1034 findings support the hypothesis that in large lakes taphonomy of chironomid
 1035 communities seems to be more complex (Yang et al., 2017; Árvá et al., 2015).
 1036
 1037



1038
 1039 **Fig. 12** Distribution grain size, organic carbon and nitrogen indices, diatom and chironomid parameters, and
 1040 selected elements and minerals in dependence to lake water depth.
 1041

1042 **5.4 Lake Bolshoe Toko as a site for palaeoclimate reconstructions**

1043 Compared to small lowland lakes of Central and Northern Yakutiá sedimentary
 1044 processes and diatoms assemblages are quite different in Bolshoe Toko. One
 1045 obvious reason for this is the lack of thaw slumps, subsidence, and other permafrost
 1046 related phenomena (Biskaborn et al., 2013b) that are typical for shallow thermokarst

1047 lake settings across northern permafrost regions (Biskaborn et al., 2016;Bouchard
1048 et al., 2016;Biskaborn et al., 2012;Schleusner et al., 2015;Biskaborn et al.,
1049 2013a;Subetto et al., 2017;Biskaborn et al., 2013b).

1050 The mineral composition in Bolshoe Toko was mainly influenced by the Utuk river
1051 and only the samples in extremely shallow areas were influenced by direct shoreline
1052 input. The grain-size signal was influenced by dissolution effects associated to
1053 organic matter and by in situ growth of diatom valves. The coarser fractions varied
1054 parallel to minerogenic compositions and water depth. Accordingly, the grain-size
1055 distribution originated from multiple processes and should only be considered as an
1056 environmental proxy in combination with biotic indicators.

1057 Diatoms were distributed mainly according to their preferential habitats. Aside of
1058 the spatial habitat conditions associated to the basin morphology, an additional
1059 principal determinant of shifting diatom assemblages in cold environments is the
1060 annual duration of lake ice-cover (Keatley et al., 2008;Smol, 1988b). **Heavily**
1061 **silicified planktonic diatoms (e.g. *Aulacoseira*) cannot survive below the lake ice-**
1062 **cover because of the absence of wind-driven water turbulence.** Nevertheless,
1063 planktonic and benthic diatom species have strategies to survive in ice-covered
1064 lakes, growing in benthic mode or attached to the bottom of the ice-cover (D'souza,
1065 2012). Hence, in many lakes, the presence or absence of the ice-cover influences
1066 blooms of different species which can result in changes of both the species
1067 distribution and the ratio of planktonic to benthic diatoms (Wang et al., 2012a).

1068 The applicability of chironomids for temperature reconstructions reveals clear
1069 spatial constraints. 22% of the taxa found in sites with riverine influence are absent
1070 or rare from the FE mean July chironomid-based temperature inference model
1071 (Nazarova et al., 2015), whereas the sum of the taxa that are rare and absent in FE
1072 data set is much lower in the central and northern littoral, sublittoral and profundal
1073 part of the lake (Fig. 4). However, low taxonomic richness of the profundal zone as
1074 well hampers palaeoclimatic inferences. The number of chironomid head capsules
1075 were generally lower here in relation to littoral sites. The highest taxonomic richness
1076 in areas influenced by lake tributaries can be explained not only by a taxonomic
1077 enrichment from the lake catchment but as well by more favorable oxygen and
1078 nutrient conditions.

1079 The applicability of $\delta^{18}\text{O}_{\text{diatom}}$ as a proxy of past hydroclimate conditions at
1080 Bolshoe Toko is generally facilitated by the fact that the main controls influencing on
1081 $\delta^{18}\text{O}_{\text{diatom}}$ in a lake are (1) the lake water temperature (T_{lake}) and (2) lake water
1082 isotope composition ($\delta^{18}\text{O}_{\text{lake}}$) (Dodd and Sharp, 2010;Leng and Barker,
1083 2006;Labeyrie, 1974;Leclerc and Labeyrie, 1987). The fractionation between lake
1084 water and biogenic opal can be calculated when comparing $\delta^{18}\text{O}_{\text{lake}}$ (mean: -18.7‰)
1085 with recent surface sediments of Bolshoe Toko lake and their respective mean
1086 $\delta^{18}\text{O}_{\text{diatom}}$ (of $+22.8\text{‰}$) using this isotope fractionation correlation between fossil

1087 diatom silica and water as determined by Leclerc and Labeyrie (1987). The mean
1088 T_{lake} can be estimated to ca. 6°C for the photic zone/diatom bloom. This estimate is
1089 at the lower end of summer temperatures between 4.8 and 12°C. The
1090 corresponding derived mean isotope fractionation factor for the system diatom
1091 silica–water $\alpha = 1.0424$ is matching the fractionation factor for fossil sediments
1092 proposed by Juillet-Leclerc and Labeyrie (1987) well ($\alpha_{(\text{silica-water})} = 1.0432$).

1093 As the lake water isotope composition ($\delta^{18}\text{O}_{\text{lake}}$) is further governed by
1094 precipitation intermittency in the catchment, $\delta^{18}\text{O}_{\text{diatom}}$ will react on changing isotopic
1095 composition in precipitation produced along the pathway of air masses to the study
1096 area, seasonality patterns and influenced by air temperature changes. Despite the
1097 observed slight spatial shifts in the surface samples $\delta^{18}\text{O}_{\text{diatom}}$ changes over time at
1098 a single site will yield insights into the air temperature and precipitation history of the
1099 area.

1100 Positive feedback mechanisms were previously described between benthic algae
1101 and chironomid larvae in benthic ecosystems (Herren et al., 2017). Chironomids in
1102 Bolshoe Toko, however, showed less significant correlations with benthic diatom
1103 species, but weak correlations with planktonic species and lake attributes
1104 associated to benthic habitats and water depth, highlighting the potential of
1105 chironomids for independent water depth and temperature reconstruction in future
1106 sediment core studies (Nazarova et al., 2011).

1107 High correlation coefficients between organic carbon and *Pliocaenicus*
1108 *bolshetokoensis* (0.66), and silt (0.65) suggest that the accumulation of organic
1109 matter, and the intermediate grain-size fraction, is to a certain degree controlled by
1110 the productivity of siliceous microalgae (Biskaborn et al., 2012). A strong
1111 contribution of plankton indicates that TOC/TN ratios can provide insights in the
1112 relative influx between land and water plants (Meyers and Teranes, 2002). The
1113 relatively weak correlation between TOC/TN ratios and water depth (0.51 r),
1114 demonstrates the accuracy limits of TOC/TN as a proxy for relative lake level
1115 changes. This is caused by transport and accumulation of allochthonous organic
1116 matter in proximity to the Utuk river. Furthermore, correlations between TOC/TN and
1117 TOC, as well as negative correlations with grain size indicators suggest diagenetic
1118 alteration (i.e. loss) of nitrogen in the surface sediments (Galman et al., 2008).

1119 The distinct difference between two samples along the subaquatic slope near the
1120 western shore (diatoms, minerals, organics) indicates redistribution of sediment.
1121 Downslope transport of surface layers over the time could lead to redistribution of
1122 old material into the deepest parts of the basin. Due to higher accumulation rates, a
1123 sediment core from the deepest part of the basin would potentially provide a higher
1124 temporal resolution, but also a higher risk of repositioned sediment layers. On top of
1125 redistribution processes, hump-shaped relations between lake depth and species
1126 diversity observed in other studies suggest that the total subfossil species

1127 assemblages is better represented at intermediate depths than at the maximum
1128 depth (Raposeiro et al., 2018). A coring position at intermediate depth in the
1129 northern shallower and sedimentologically calm part of the basin would enable the
1130 tracking of different intensities of river influence and glacial activity using sediment-
1131 geochemical indicators and offers greater chances of undisturbed successions of
1132 bioindicator time series.
1133

1134 **6 Conclusions**

1135 Our study on the within-lake variance of environmental indicator data and its
1136 attribution to habitat factors improves the understanding of lake-internal filters
1137 between environmental forcing and the resulting sediment parameters of Lake
1138 Bolshoe Toko and comparable boreal, cold, and deep lakes. We found that the
1139 spatial variabilities of biotic ecosystem components are mainly explained by static
1140 habitat preferences as water depth and river distance. Abiotic sediment features are
1141 not symmetrically distributed in the basin but vary along restricted areas of
1142 differential environmental forcings (e.g. river input, rocky shore, steep shore, shallow
1143 shore). They depend, in addition to water depth and riverine activity, to multiple
1144 interacting factor, such as catchment characteristics, geochemical sediment
1145 diagenesis and hydrochemical dynamics. Our main findings can be highlighted as
1146 follows:

- 1147
- 1148 • The lake water of Bolshoe Toko can be characterized as Ca-Mg-HCO₃-Type
1149 water. It is well saturated in O₂, neutral to slightly acidic, showing a low
1150 conductivity and corresponding ion concentrations suggesting unpolluted
1151 freshwater conditions. Lake Bolshoe Toko is likely a cold, polymictic,
1152 oligotrophic, open through-flow lake system and due to all stated aspects
1153 regarded as an undisturbed ecosystem.
- 1154 • Water depth is a strong factor explaining the variability of diatoms and
1155 chironomids. The proportions of planktonic to benthic diatoms as well as
1156 profundal to littoral chironomids serve as a reliable lake level proxy.
- 1157 • The diatom assemblage is dominated by planktonic species, i.e. *Pliocaenicus*
1158 *bolshetokoensis*, which is unique for this lake, and more common plankton
1159 such as *Cyclotella* and *Aulacoseira*, as well as non-planktonic taxa, such as
1160 *Achnantheidium*. Diatom species richness and diversity is higher in surface
1161 sediments in the northern part of the basin, associated to shallower waters
1162 and the availability of benthic and periphytic niches.
- 1163 • The $\delta^{18}\text{O}_{\text{diatom}}$ values ($22.8 \pm 0.6\text{‰}$) show slight spatial variations with higher
1164 values in the deeper south-western part of the lake probably related to water
1165 temperature differences in the photic zone during the main diatom bloom.

1166 The silica–water fractionation is suitable for further downcore investigations
1167 for assessing paleo-hydrological information and potential air-temperature
1168 changes in the region.

- 1169 • The water of Bolshoe Toko is well mixed and does not show significant
1170 isotopic stratification apart from lake ice-cover formation where thermal
1171 stratification prevents mixing. The isotopic lake water composition ($\delta^{18}\text{O} =$
1172 $18.2 \pm 0.2 \text{ ‰}$) correspond with the GMWL and do not show evaporative
1173 enrichment. Both isotopic and hydrochemical data indicate atmospheric
1174 precipitation (and meltwater run-off) as the main water source. Accordingly,
1175 $\delta^{18}\text{O}_{\text{lakewater}}$ is directly linked to $\delta^{18}\text{O}_{\text{precipitation}}$.
- 1176 • The highest amount of the chironomid taxa underrepresented in the FE
1177 training set used for palaeoclimate inference was found close to the Utuk
1178 river and at southern littoral and profundal sites. Poor chironomid
1179 communities from the deep profundal zone would also hamper palaeoclimate
1180 reconstruction. Cold-stenotherm chironomid taxa were influenced by river
1181 proximity while taxa preferring warm conditions were more frequent at
1182 shallow littorals of the lake.
- 1183 • Weak negative correlation between mean grain size and water depth is
1184 explain by end-members revealing influences of river input and diatom valves
1185 in the grain-size composition.
- 1186 • Observed TOC values (mean 4.9 %) and TOC/TN ratios indicate strong
1187 allochthonous supply of organic matter from the Utuk river. $\delta^{13}\text{C}$ (mean -26.8
1188 ‰) indicate dominance of C_3 plants and phytoplankton in the bulk organic
1189 matter fraction.
- 1190 • Elemental (XRF) data and mineral (XRD) distribution is influenced by the
1191 metamorphic lithology of the Stanovoy mountain range. Ratios of minerals
1192 relative to quartz decrease from the Utuk river towards the northern lake
1193 basin. Ti correlates well with mean grain size. There is no clear pattern in
1194 Mn/Fe ratios, due to mixture of allochthonous elements and differential
1195 intensities of redox processes in the lake basin.

1196

1197 **Data Availability**

1198 All data used in this study is available online at PANGAEA (DOI: XXXXXXwill be
1199 provided during review processXXXXXXX)

1200

1201 **Supplement**

1202 The supplementary material related to this study is available online at XXXXwill
1203 be included by CopernicusXXXX.

1204 **Author contributions**

1205 BKB conceived the study concept, conducted or led the laboratory analyses and
1206 led the writing of the manuscript. LN conducted statistical analyses and contributed
1207 with ecological chironomid expertise. LAP led the Russian team during field work
1208 and contributed with ecological diatom expertise. LS conducted chironomid analysis.
1209 KF conducted diatom analyses. HM conducted water chemistry analyses. BC
1210 analysed diatom opal oxygen isotopes. SV conducted the XRF analysis. RG and EZ
1211 retrieved surface samples during field work and helped with translation of Russian
1212 literature and geographical expertise of the study area. RW conducted grain-size
1213 analyses including end-member modelling. GS conducted XRD analyses. BD was
1214 the leader of German expedition team and contributed with sedimentological
1215 expertise.
1216

1217 **Competing interests**

1218 The authors declare that they have no conflict of interest.

1219 **Acknowledgements**

1220 The expedition Yakutia 2013 was financed and conducted by the Alfred Wegener
1221 Institute Helmholtz Centre for Polar and Marine Research in Potsdam, Germany in
1222 collaboration with the North Eastern Federal University in Yakutsk, Russia. Parts of
1223 the study was financed by the Federal Ministry of Education and Research (BMBF)
1224 in the PALMOD project (#01LP1510D) and grant #5.2711.2017/4.6, the Russian
1225 Foundation for Basic Research (RFBR grant #18-45-140053 r_a), and the Project of
1226 the North-Eastern Federal University (Regulation SMK-P-1/2-242-17 ver. 2.0, order
1227 No. 494-OD), Russian Science Foundation (#16-17-10118), and Deutsche
1228 Forschungsgemeinschaft DFG (#NA 760/5-1 and #DI 655/9-1). We thank Almut
1229 Dressler and Clara Biskaborn for help with diatom microscopy and Thomas Löffler
1230 for help with mineral analyses. We thank the anonymous reviewers for their
1231 voluntary efforts to assure the quality of this study.
1232
1233

1234 **References**

1235 Adrian, R., O'Reilly, C. M., Zagarese, H., Baines, S. B., Hessen, D. O., Keller, W., Livingstone, D. M.,
1236 Sommaruga, R., Straile, D., Van Donk, E., Weyhenmeyer, G. A., and Winder, M.: Lakes as sentinels
1237 of climate change, *Limnology and Oceanography*, 54, 2283-2297,
1238 10.4319/lo.2009.54.6_part_2.2283, 2009.

1239 Ali, A., Frouz, J., and Lobinske, R. J.: Spatio-temporal effects of selected physico-chemical variables
1240 of water, algae and sediment chemistry on the larval community of nuisance Chironomidae (Diptera)
1241 in a natural and a man-made lake in central Florida, *Hydrobiologia*, 470, 181-193, 2002.

- 1242 AMAP: Snow, Water, Ice and Permafrost in the Arctic (SWIPA) 2017, Oslo, Norway, 1-269, 2017.
- 1243 Anderson, N. J.: Variability of diatom concentrations and accumulation rates in sediments of a small
1244 lake basin, *Limnology and Oceanography*, 35, 497-508, 1990.
- 1245 Anderson, N. J., Korsman, T., and Renberg, I.: Spatial heterogeneity of diatom stratigraphy in varved
1246 and non-varved sediments of a small, boreal-forest lake, *Aquatic Sciences*, 56, 40-58,
1247 10.1007/bf00877434, 1994.
- 1248 Anderson, N. J.: Diatoms, temperature and climatic change, *European Journal of Phycology*, 35,
1249 307-314, doi:null, 2000.
- 1250 Árva, D., Tóth, M., Horváth, H., Nagy, S. A., and Specziár, A.: The relative importance of spatial and
1251 environmental processes in distribution of benthic chironomid larvae within a large and shallow lake,
1252 *Hydrobiologia*, 742, 249-266, 2015.
- 1253 Bailey, H. L., Henderson, A. C. G., Sloane, H. J., Snelling, A., Leng, M. J., and Kaufman, D. S.: The
1254 effect of species on lacustrine $\delta^{18}\text{O}$ diatom and its implications for palaeoenvironmental
1255 reconstructions, *Journal of Quaternary Science*, 29, 393-400, 10.1002/jqs.2711, 2014.
- 1256 Barinova, S., Nevo, E., and Bragina, T.: Ecological assessment of wetland ecosystems of northern
1257 Kazakhstan on the basis of hydrochemistry and algal biodiversity, 2011.
- 1258 Battarbee, R. W., and Kneen, M. J.: The use of electronically counted microspheres in absolute
1259 diatom analysis, *Limnology and Oceanography*, 27, 184-188, 1982.
- 1260 Battarbee, R. W., Jones, V. J., Flower, R. J., Cameron, N. G., Bennion, H., Carvalho, L., and
1261 Juggins, S.: Diatoms, in: *Tracking Environmental Change Using Lake Sediments*, edited by: Smol, J.
1262 P., Birks, H. J. B., and Last, W. M., Kluwer Academic Publishers, Dordrecht, Netherlands, 155-202,
1263 2001.
- 1264 Bennion, H., Sayer, C. D., Tibby, J., and Carrick, H. J.: Diatoms as Indicators of Environmental
1265 Change in Shallow Lakes, in: *The Diatoms: Application for the Environmental and Earth Sciences*,
1266 edited by: Smol, J. P., and Stoermer, E. F., Cambridge University Press, Cambridge, 152-173, 2010.
- 1267 Birks, H. J. B.: Quantitative palaeoenvironmental reconstructions, *Statistical modelling of quaternary
1268 science data. Technical guide*, 5, 161-254, 1995.
- 1269 Biskaborn, B., Herzschuh, U., Bolshiyarov, D., Savelieva, L., Zibulski, R., and Diekmann, B.: Late
1270 Holocene thermokarst variability inferred from diatoms in a lake sediment record from the Lena Delta,
1271 Siberian Arctic, *Journal of Paleolimnology*, 49, 155-170, 10.1007/s10933-012-9650-1, 2013a.
- 1272 Biskaborn, B., Herzschuh, U., Bolshiyarov, D., Schwamborn, G., and Diekmann, B.: Thermokarst
1273 Processes and Depositional Events in a Tundra Lake, Northeastern Siberia, *Permafrost and
1274 Periglacial Processes*, 24, 160-174, 10.1002/ppp.1769, 2013b.
- 1275 Biskaborn, B. K., Herzschuh, U., Bolshiyarov, D., Savelieva, L., and Diekmann, B.: Environmental
1276 variability in northeastern Siberia during the last similar to 13,300 yr inferred from lake diatoms and
1277 sediment-geochemical parameters, *Palaeogeography Palaeoclimatology Palaeoecology*, 329, 22-36,
1278 10.1016/j.palaeo.2012.02.003, 2012.
- 1279 Biskaborn, B. K., Subetto, D. A., Savelieva, L. A., Vakhrameeva, P. S., Hansche, A., Herzschuh, U.,
1280 Klemm, J., Heinecke, L., Pestryakova, L. A., Meyer, H., Kuhn, G., and Diekmann, B.: Late
1281 Quaternary vegetation and lake system dynamics in north-eastern Siberia: Implications for seasonal
1282 climate variability, *Quaternary Science Reviews*, 147, 406-421, 10.1016/j.quascirev.2015.08.014,
1283 2016.

- 1284 Biskaborn, B. K., Smith, S. L., Noetzli, J., Matthes, H., Vieira, G., Streletskiy, D. A., Schoeneich, P.,
 1285 Romanovsky, V. E., Lewkowicz, A. G., Abramov, A., Allard, M., Boike, J., Cable, W. L., Christiansen,
 1286 H. H., Delaloye, R., Diekmann, B., Drozdov, D., Etzelmüller, B., Grosse, G., Guglielmin, M.,
 1287 Ingeman-Nielsen, T., Isaksen, K., Ishikawa, M., Johansson, M., Johannsson, H., Joo, A., Kaverin, D.,
 1288 Kholodov, A., Konstantinov, P., Kröger, T., Lambiel, C., Lanckman, J.-P., Luo, D., Malkova, G.,
 1289 Meiklejohn, I., Moskalenko, N., Oliva, M., Phillips, M., Ramos, M., Sannel, A. B. K., Sergeev, D.,
 1290 Seybold, C., Skryabin, P., Vasiliev, A., Wu, Q., Yoshikawa, K., Zheleznyak, M., and Lantuit, H.:
 1291 Permafrost is warming at a global scale, *Nature Communications*, 10, 264, 10.1038/s41467-018-
 1292 08240-4, 2019.
- 1293 Bouchard, F., Turner, K. W., MacDonald, L. A., Deakin, C., White, H., Farquharson, N., Medeiros, A.
 1294 S., Wolfe, B. B., Hall, R. I., Pienitz, R., and Edwards, T. W. D.: Vulnerability of shallow subarctic
 1295 lakes to evaporate and desiccate when snowmelt runoff is low, *Geophysical Research Letters*, 40,
 1296 6112-6117, 10.1002/2013gl058635, 2013.
- 1297 Bouchard, F., MacDonald, L. A., Turner, K. W., Thienpont, J. R., Medeiros, A. S., Biskaborn, B. K.,
 1298 Korosi, J., Hall, R. I., Pienitz, R., and Wolfe, B. B.: Paleolimnology of thermokarst lakes: a window
 1299 into permafrost landscape evolution, *Arctic Science*, 10.1139/AS-2016-0022, 2016.
- 1300 Bracht-Flyr, B., and Fritz, S. C.: Synchronous climatic change inferred from diatom records in four
 1301 western Montana lakes in the U.S. Rocky Mountains, *Quaternary Research*, 77, 456-467,
 1302 10.1016/j.yqres.2011.12.005, 2012.
- 1303 Brandriss, M. E., O'Neil, J. R., Edlund, M. B., and Stoermer, E. F.: Oxygen Isotope Fractionation
 1304 Between Diatomaceous Silica and Water, *Geochimica et Cosmochimica Acta*, 62, 1119-1125,
 1305 10.1016/S0016-7037(98)00054-4, 1998.
- 1306 Brooks, S. J., and Birks, H. J. B.: Chironomid-inferred air temperatures from Lateglacial and
 1307 Holocene sites in north-west Europe: progress and problems, *Quaternary Science Reviews*, 20,
 1308 1723-1741, 2001.
- 1309 Brooks, S. J., Langdon, P. G., and Heiri, O.: The identification and use of Palaeartic Chironomidae
 1310 larvae in palaeoecology, *Quaternary Research Association*, 2007.
- 1311 Chaplignin, B., Meyer, H., Friedrichsen, H., Marent, A., Sohns, E., and Hubberten, H. W.: A high-
 1312 performance, safer and semi-automated approach for the δ 18O analysis of diatom silica and new
 1313 methods for removing exchangeable oxygen, *Rapid Communications in Mass Spectrometry*, 24,
 1314 2655-2664, 2010.
- 1315 Chaplignin, B.: From method development to climate reconstruction - oxygen isotope analysis of
 1316 biogenic silica from Lake El'gygytgyn, NE Siberia, PhD thesis, Alfred Wegener Institute for Polar and
 1317 Marine Research, University of Potsdam, Potsdam, 196 pp., 2011.
- 1318 Chaplignin, B., Meyer, H., Bryan, A., Snyder, J., and Kemnitz, H.: Assessment of purification and
 1319 contamination correction methods for analysing the oxygen isotope composition from biogenic silica,
 1320 *Chemical Geology*, 300, 185-199, 10.1016/j.chemgeo.2012.01.004, 2012.
- 1321 Cohen, A. S.: *Palaeolimnology - The History and Evolution of Lake Systems*, Oxford University
 1322 Press, Oxford, 500 pp., 2003.
- 1323 Cremer, H., and Van de Vijver, B.: On *Pliocaenicus costatus* (Bacillariophyceae) in Lake El'gygytgyn,
 1324 East Siberian, *European Journal of Phycology*, 41, 169-178, 10.1080/09670260600621932, 2006.
- 1325 D'souza, N. A.: *Psychrophilic diatoms in ice-covered lake Erie*, Bowling Green State University, 158
 1326 pp., 2012.
- 1327 Dansgaard, W.: Stable Isotopes in Precipitation, *Tellus*, 16, 436-468, 1964.

- 1328 Dietze, E., Hartmann, K., Diekmann, B., Ijmker, J., Lehmkuhl, F., Opitz, S., Stauch, G., Wünnemann,
1329 B., and Borchers, A.: An end-member algorithm for deciphering modern detrital processes from lake
1330 sediments of Lake Donggi Cona, NE Tibetan Plateau, China, *Sedimentary Geology*, 243–244, 169-
1331 180, 10.1016/j.sedgeo.2011.09.014, 2012.
- 1332 Dodd, J. P., and Sharp, Z. D.: A laser fluorination method for oxygen isotope analysis of biogenic
1333 silica and a new oxygen isotope calibration of modern diatoms in freshwater environments,
1334 *Geochimica et Cosmochimica Acta*, 74, 1381-1390, 2010.
- 1335 Dodd, J. P., Sharp, Z. D., Fawcett, P. J., Brearley, A. J., and McCubbin, F. M.: Rapid post-mortem
1336 maturation of diatom silica oxygen isotope values, *Geochemistry, Geophysics, Geosystems*, 13,
1337 10.1029/2011GC004019, 2012.
- 1338 Douglas, M. S. V., and Smol, J. P.: Paleolimnological Significance of observed Distribution Patterns of
1339 Chrysophyte Cysts in Arctic Pond Environments, *Journal of Paleolimnology*, 13, 79-83, 1995.
- 1340 Douglas, M. S. V., and Smol, J. P.: Freshwater Diatoms as Indicators of Environmental Change in
1341 the High Arctic, in: *The Diatoms: Application for the Environmental and Earth Sciences*, edited by:
1342 Smol, J. P., and Stoermer, E. F., Cambridge University Press, Cambridge, 249-266, 2010.
- 1343 Earle, J. C., Duthie, H. C., Glooschenko, W. A., and Hamilton, P. B.: Factors affecting the spatial-
1344 distribution of diatoms on the surface sediments of 3 Precambrian shield lakes, *Canadian Journal of*
1345 *Fisheries and Aquatic Sciences*, 45, 469-478, 10.1139/f88-056, 1988.
- 1346 Elger, K., Biskaborn, B. K., Pampel, H., and Lantuit, H.: Open research data, data portals and data
1347 publication—an introduction to the data curation landscape, *Polarforschung*, 85, 119-133, 2016.
- 1348 Flower, R. J., and Ryves, D. B.: Diatom preservation: differential preservation of sedimentary diatoms
1349 in two saline lakes, *Acta Botanica Croatica*, 68, 381-399, 2009.
- 1350 Galman, V., Rydberg, J., de-Luna, S. S., Bindler, R., and Renberg, I.: Carbon and nitrogen loss rates
1351 during aging of lake sediment: Changes over 27 years studied in varved lake sediment, *Limnology*
1352 *and Oceanography*, 53, 1076-1082, DOI 10.4319/lo.2008.53.3.1076, 2008.
- 1353 Gavin, D. G., Henderson, A. C. G., Westover, K. S., Fritz, S. C., Walker, I. R., Leng, M. J., and Hu, F.
1354 S.: Abrupt Holocene climate change and potential response to solar forcing in western Canada,
1355 *Quaternary Science Reviews*, 30, 1243-1255, 10.1016/j.quascirev.2011.03.003, 2011.
- 1356 Gavrilova, K.: *Climate and Permafrost, Permafrost and Periglacial Processes*, 4, 99-111, 1993.
- 1357 Genkal, S., Gabyshev, V., Kulilovskiy, M., and Kuznetsova, I.: *Pliocaenicus bolshetokoensis*—a new
1358 species from Lake Bolshoe Toko (Yakutia, Eastern Siberia, Russia), *Diatom Research*, 1-9, 2018.
- 1359 Gingele, F. X., De Deckker, P., and Hillenbrand, C.-D.: Clay mineral distribution in surface sediments
1360 between Indonesia and NW Australia—source and transport by ocean currents, *Marine Geology*,
1361 179, 135-146, 2001.
- 1362 Gushulak, C. A. C., Laird, K. R., Bennett, J. R., and Cumming, B. F.: Water depth is a strong driver of
1363 intra-lake diatom distributions in a small boreal lake, *Journal of Paleolimnology*, 58, 231-241,
1364 10.1007/s10933-017-9974-y, 2017.
- 1365 Hakanson, L.: Influence of Wind, Fetch, and Water Depth on Distribution of Sediments in Lake
1366 Vanern, Sweden, *Canadian Journal of Earth Sciences*, 14, 397-412, 10.1139/e77-040, 1977.
- 1367 Heggen, M. P., Birks, H. H., Heiri, O., Grytnes, J. D., and Birks, H. J. D.: Are fossil assemblages in a
1368 single sediment core from a small lake representative of total deposition of mite, chironomid, and
1369 plant macrofossil remains?, *Journal of Paleolimnology*, 48, 669-691, 2012.

- 1370 Heinecke, L., Mischke, S., Adler, K., Barth, A., Biskaborn, B. K., Plessen, B., Nitze, I., Kuhn, G.,
 1371 Rajabov, I., and Herzsuh, U.: Climatic and limnological changes at Lake Karakul (Tajikistan) during
 1372 the last similar to 29 cal ka, *Journal of Paleolimnology*, 58, 317-334, 10.1007/s10933-017-9980-0,
 1373 2017.
- 1374 Heiri, O., and Lotter, A. F.: Effect of low count sums on quantitative environmental reconstructions:
 1375 an example using subfossil chironomids, *Journal of Paleolimnology*, 26, 343-350, 2001.
- 1376 Heiri, O., Brooks, S. J., Renssen, H., Bedford, A., Hazekamp, M., Ilyashuk, B., Jeffers, E. S., Lang,
 1377 B., Kirilova, E., and Kuiper, S.: Validation of climate model-inferred regional temperature change for
 1378 late-glacial Europe, *Nature communications*, 5, 4914, 2014.
- 1379 Heling, C. L., Stelzer, R. S., Drecktrah, H. G., and Koenigs, R. P.: Spatial variation of benthic
 1380 invertebrates at the whole-ecosystem scale in a large eutrophic lake, *Freshwater Science*, 37, 605-
 1381 617, 10.1086/699386, 2018.
- 1382 Herren, C. M., Webert, K. C., Drake, M. D., Vander Zanden, M. J., Einarsson, A., Ives, A. R., and
 1383 Gratton, C.: Positive feedback between chironomids and algae creates net mutualism between
 1384 benthic primary consumers and producers, *Ecology*, 98, 447-455, 10.1002/ecy.1654, 2017.
- 1385 Herzsuh, U., Pestryakova, L. A., Savelieva, L. A., Heinecke, L., Boehmer, T., Biskaborn, B. K.,
 1386 Andreev, A., Ramisch, A., Shinneman, A. L. C., and Birks, H. J. B.: Siberian larch forests and the ion
 1387 content of thaw lakes form a geochemically functional entity, *Nature Communications*, 4,
 1388 10.1038/ncomms3408, 2013.
- 1389 Hilton, J., Lishman, J. P., and Allen, P. V.: The dominant processes of sediment distribution and
 1390 focusing in a small, eutrophic, monomictic lake, *Limnology and Oceanography*, 31, 125-133, 1986.
- 1391 Hoff, U., Biskaborn, B. K., Dirksen, V. G., Dirksen, O., Kuhn, G., Meyer, H., Nazarova, L., Roth, A.,
 1392 and Diekmann, B.: Holocene environment of Central Kamchatka, Russia: Implications from a multi-
 1393 proxy record of Two-Yurts Lake, *Global and Planetary Change*, 134, 101-117,
 1394 10.1016/j.gloplacha.2015.07.011, 2015.
- 1395 Hofmann, W.: Zur taxonomie und palökologie subfossiler Chironomiden (Dipt.) in seesedimenten,
 1396 *Ergebnisse der Limnologie*, 1971.
- 1397 Huang, J., Zhang, X., Zhang, Q., Lin, Y., Hao, M., Luo, Y., Zhao, Z., Yao, Y., Chen, X., Wang, L.,
 1398 Nie, S., Yin, Y., Xu, Y., and Zhang, J.: Recently amplified arctic warming has contributed to a
 1399 continual global warming trend, *Nature Climate Change*, 7, 875-879, 10.1038/s41558-017-0009-5,
 1400 2017.
- 1401 Imaeva, L., Imaev, V., Koz'min, B., and Mackey, K.: Formation dynamics of fault-block structures in
 1402 the eastern segment of the Baikal-Stanovoi seismic belt, *Izvestiya-Physics of the Solid Earth*, 45,
 1403 1006-1011, 10.1134/S1069351309110081, 2009.
- 1404 Kalinkina, N., and Belkina, N.: Dynamics of benthic communities state and the sediment chemical
 1405 composition in Lake Onega under the influence of anthropogenic and natural factors, *Principy*
 1406 *èkologii*, 7, 56-74, 10.15393/j1.art.2018.7643, 2018.
- 1407 Kalugin, I., Daryin, A., Smolyaninova, L., Andreev, A., Diekmann, B., and Khlystov, O.: 800-yr-long
 1408 records of annual air temperature and precipitation over southern Siberia inferred from Teletskoye
 1409 Lake sediments, *Quaternary Research*, 67, 400-410, 10.1016/j.yqres.2007.01.007, 2007.
- 1410 Keatley, B. E., Douglas, M. S. V., and Smol, J. P.: Prolonged ice cover dampens diatom community
 1411 responses to recent climatic change in High Arctic lakes, *Arctic Antarctic and Alpine Research*, 40,
 1412 364-372, 10.1657/1523-0430(06-068)[keatley]2.0.co;2, 2008.

- 1413 Kiene, U., and Kumke, T.: Combining ordination techniques and geostatistics to determine the
1414 patterns of diatom distributions at Lake Lama, Central Siberia, *Journal of Paleolimnology*, 28, 181-
1415 194, 2002.
- 1416 Kingston, J. C., Lowe, R. L., Stoermer, E. F., and Ladewski, T. B.: Spatial and Temporal Distribution
1417 of Benthic Diatoms in Northern Lake Michigan, *Ecology*, 64, 1566-1580, 10.2307/1937511, 1983.
- 1418 Konstantinov, A. F.: Problems of Water-Resources Development in Southern Yakutia (in Russian),
1419 *Yaf Sib. Otd. Akad., Nauk SSSR, Yakutsk*, 136 pp., 1986.
- 1420 Konstantinov, A. F.: Environmental problems of lake Bolshoe Toko (in Russian), *Lakes of Cold*
1421 *Environments, part V: Resource Study, Resource Use, Ecology and Nature Protection Issue*,
1422 *Yakutsk, Russia*, 2000, 85-93,
- 1423 Kornilov, B. A.: Relief: The southeast suburbs of Aldan Mountains (in Russian), Publishing House of
1424 Academy of Sciences of the USSR, Moscow, 1962.
- 1425 Kovalenko, K. E., Thomaz, S. M., and Warfe, D. M.: Habitat complexity: approaches and future
1426 directions, *Hydrobiologia*, 685, 1-17, 10.1007/s10750-011-0974-z, 2012.
- 1427 Krammer, K., and Lange-Bertalot, H.: *Bacillariophyceae Band 2/2, Süßwasserflora von Mitteleuropa*,
1428 2, Gustav Fischer Verlag, Stuttgart, 1986-1991.
- 1429 Labeyrie, L.: New approach to surface seawater palaeotemperatures using 18O/16O ratios in silica
1430 of diatom frustules, *Nature*, 248, 40-42, 10.1038/248040a0, 1974.
- 1431 Lange-Bertalot, H., and Metzeltin, D.: Indicators of Oligotrophy, *Iconographia Diatomologica*, 2,
1432 Koeltz Scientific Books, 390 pp., 1996.
- 1433 Lange-Bertalot, H., and Genkal, S. I.: Diatomeen aus Sibirien I, *Iconographia Diatomologica*, 6,
1434 Koeltz Scientific Books, 271 pp., 1999.
- 1435 Lange-Bertalot, H., Hofmann, G., and Werum, M.: *Diatomeen im Süßwasser - Benthos von*
1436 *Mitteleuropa*, Ganter Verlag, 908 pp., 2011.
- 1437 Leclerc, A. J., and Labeyrie, L.: Temperature dependence of the oxygen isotopic fractionation
1438 between diatom silica and water, *Earth and Planetary Science Letters*, 84, 69-74, 1987.
- 1439 Leng, M. J., and Barker, P. A.: A review of the oxygen isotope composition of lacustrine diatom silica
1440 for palaeoclimate reconstruction, *Earth-Science Reviews*, 75, 5, 2006.
- 1441 Livingstone, D. M., Lotter, A. F., and Walkery, I. R.: The decrease in summer surface water
1442 temperature with altitude in Swiss Alpine lakes: a comparison with air temperature lapse rates, *Arctic*,
1443 *Antarctic, and Alpine Research*, 31, 341-352, 1999.
- 1444 Luoto, T. P.: Spatial uniformity in depth optima of midges: evidence from sedimentary archives of
1445 shallow Alpine and boreal lakes, *Journal of Limnology*, 71, e24-e24, 2012.
- 1446 Luoto, T. P., and Ojala, A. E. K.: Controls of climate, catchment erosion and biological production on
1447 long-term community and functional changes of chironomids in High Arctic lakes (Svalbard),
1448 *Palaeogeography Palaeoclimatology Palaeoecology*, 505, 63-72, 10.1016/j.palaeo.2018.05.026,
1449 2018.
- 1450 Mayr, C., Lücke, A., Stichler, W., Trimborn, P., Ercolano, B., Oliva, G., Ohlendorf, C., Soto, J., Fey,
1451 M., and Haberzettl, T.: Precipitation origin and evaporation of lakes in semi-arid Patagonia
1452 (Argentina) inferred from stable isotopes ($\delta^{18}\text{O}$, $\delta^2\text{H}$), *Journal of Hydrology*, 334, 53-63, 2007.

- 1453 Melles, M., Brigham-Grette, J., Minyuk, P. S., Nowaczyk, N. R., Wennrich, V., DeConto, R. M.,
 1454 Anderson, P. M., Andreev, A. A., Coletti, A., Cook, T. L., Haltia-Hovi, E., Kukkonen, M., Lozhkin, A.
 1455 V., Rosén, P., Tarasov, P., Vogel, H., and Wagner, B.: 2.8 Million Years of Arctic Climate Change
 1456 from Lake El'gygytyn, NE Russia, *Science*, 337, 315, 10.1126/science.1222135, 2012.
- 1457 Merlivat, L., and Jouzel, J.: Global climatic interpretation of the deuterium-oxygen 18 relationship for
 1458 precipitation, *Journal of Geophysical Research: Oceans*, 84, 5029-5033, 1979.
- 1459 Meyer, D., Tachikawa, T., Kaku, M., Iwasaki, A., Gesch, D., Oimoen, M., Zheng, Z., Danielson, J.,
 1460 Krieger, T., and Curtis, W.: ASTER global digital elevation model version 2—summary of validation
 1461 results, Japan-US ASTER Science Team, 1-26, 2011.
- 1462 Meyer, H., Schönicke, L., Wand, U., Hubberten, H.-W., and Friedrichsen, H.: Isotope studies of
 1463 hydrogen and oxygen in ground ice—experiences with the equilibration technique, *Isotopes in
 1464 Environmental and Health Studies*, 36, 133-149, 2000.
- 1465 Meyer, H., Chaplignin, B., Hoff, U., Nazarova, L., and Diekmann, B.: Oxygen isotope composition of
 1466 diatoms as Late Holocene climate proxy at Two-Yurts Lake, Central Kamchatka, Russia, *Global and
 1467 Planetary Change*, 134, 118-128, 2015.
- 1468 Meyers, P. A., and Teranes, J. L.: Sediment organic matter, in: *Tracking Environmental Change
 1469 using Lake Sediments. Volume 2: Physical and Geochemical Methods*, edited by: Last, W. M., and
 1470 Smol, J. P., Kluwer Academic Publisher, Dordrecht, 239-269, 2002.
- 1471 Meyers, P. A.: Applications of organic geochemistry to paleolimnological reconstructions: a summary
 1472 of examples from the Laurentian Great Lakes, *Organic Geochemistry*, 34, 261-289, 2003.
- 1473 Miller, G. H., Brigham-Grette, J., Alley, R. B., Anderson, L., Bauch, H. A., Douglas, M. S. V.,
 1474 Edwards, M. E., Elias, S. A., Finney, B. P., Fitzpatrick, J. J., Funder, S. V., Herbert, T. D., Hinzman,
 1475 L. D., Kaufman, D. S., MacDonald, G. M., Polyak, L., Robock, A., Serreze, M. C., Smol, J. P.,
 1476 Spielhagen, R., White, J. W. C., Wolfe, A. P., and Wolff, E. W.: Temperature and precipitation history
 1477 of the Arctic, *Quaternary Science Reviews*, 29, 1679-1715, DOI: 10.1016/j.quascirev.2010.03.001,
 1478 2010.
- 1479 Moschen, R., Lucke, A., and Schleser, G. H.: Sensitivity of biogenic silica oxygen isotopes to
 1480 changes in surface water temperature and palaeoclimatology, *Geophysical Research Letters*, 32,
 1481 L07708
 1482 10.1029/2004gl022167, 2005.
- 1483 Naeher, S., Gilli, A., North, R. P., Hamann, Y., and Schubert, C. J.: Tracing bottom water
 1484 oxygenation with sedimentary Mn/Fe ratios in Lake Zurich, Switzerland, *Chemical Geology*, 352,
 1485 125-133, 10.1016/j.chemgeo.2013.06.006, 2013.
- 1486 Nazarova, L., Pestryakova, L., Ushnitskaya, L., and Hubberten, H.-W.: Chironomids (Diptera:
 1487 Chironomidae) in lakes of central Yakutia and their indicative potential for paleoclimatic research,
 1488 *Contemporary Problems of Ecology*, 1, 335, 2008.
- 1489 Nazarova, L., Herzschuh, U., Wetterich, S., Kumke, T., and Pestryakova, L.: Chironomid-based
 1490 inference models for estimating mean July air temperature and water depth from lakes in Yakutia,
 1491 northeastern Russia, *Journal of Paleolimnology*, 45, 57-71, 2011.
- 1492 Nazarova, L., Self, A. E., Brooks, S. J., van Hardenbroek, M., Herzschuh, U., and Diekmann, B.:
 1493 Northern Russian chironomid-based modern summer temperature data set and inference models,
 1494 *Global and Planetary Change*, 134, 10-25, 2015.
- 1495 Nazarova, L., Grebennikova, T. A., Razjigaeva, N. G., Ganzey, L. A., Belyanina, N. I., Arslanov, K.
 1496 A., Kaistrenko, V. M., Gorbunov, A. O., Kharlamov, A. A., and Rudaya, N.: Reconstruction of

- 1497 Holocene environmental changes in Southern Kurils (North-Western Pacific) based on palaeolake
1498 sediment proxies from Shikotan Island, *Global and Planetary Change*, 159, 25-36, 2017a.
- 1499 Nazarova, L. B., Semenov, V. F., Sabirov, R. M., and Efimov, I. Y.: The state of benthic communities
1500 and water quality evaluation in the Cheboksary Reservoir, *Water Resources*, 31, 316-322, 2004.
- 1501 Nazarova, L. B., Self, A. E., Brooks, S. J., Solovieva, N., Syrykh, L. S., and Dauvalter, V. A.:
1502 Chironomid fauna of the lakes from the Pechora river basin (east of European part of Russian Arctic):
1503 Ecology and reconstruction of recent ecological changes in the region, *Contemporary Problems of
1504 Ecology*, 10, 350-362, 10.1134/s1995425517040059, 2017b.
- 1505 New, M., Lister, D., Hulme, M., and Makin, I.: A high-resolution data set of surface climate over
1506 global land areas, *Climate research*, 21, 1-25, 2002.
- 1507 Palagushkina, O., Wetterich, S., Biskaborn, B. K., Nazarova, L., Schirrmeister, L., Lenz, J.,
1508 Schwamborn, G., and Grosse, G.: Diatom records and tephra mineralogy in pingo deposits of
1509 Seward Peninsula, Alaska, *Palaeogeography, Palaeoclimatology, Palaeoecology*, 2017.
- 1510 Palagushkina, O. V., Nazarova, L. B., Wetterich, S., and Schirrmeister, L.: Diatoms of modern bottom
1511 sediments in Siberian arctic, *Contemporary Problems of Ecology*, 5, 413-422,
1512 10.1134/s1995425512040105, 2012.
- 1513 Paul, C. A., Rühland, K. M., and Smol, J. P.: Diatom-inferred climatic and environmental changes
1514 over the last 9000 years from a low Arctic (Nunavut, Canada) tundra lake, *Palaeogeography
1515 Palaeoclimatology Palaeoecology*, 291, 205-216, 10.1016/j.palaeo.2010.02.030, 2010.
- 1516 Pepin, N., Bradley, R. S., Diaz, H. F., Baraer, M., Caceres, E. B., Forsythe, N., Fowler, H.,
1517 Greenwood, G., Hashmi, M. Z., Liu, X. D., Miller, J. R., Ning, L., Ohmura, A., Palazzi, E., Rangwala,
1518 I., Schoner, W., Severskiy, I., Shahgedanova, M., Wang, M. B., Williamson, S. N., Yang, D. Q., and
1519 Mt Res Initiative, E. D. W. W. G.: Elevation-dependent warming in mountain regions of the world,
1520 *Nature Climate Change*, 5, 424-430, 10.1038/nclimate2563, 2015.
- 1521 Pestryakova, L. A., Herzschuh, U., Wetterich, S., and Ulrich, M.: Present-day variability and
1522 Holocene dynamics of permafrost-affected lakes in central Yakutia (Eastern Siberia) inferred from
1523 diatom records, *Quaternary Science Reviews*, 51, 56-70, 2012.
- 1524 Pestryakova, L. A., Herzschuh, U., Gorodnichev, R., and Wetterich, S.: The sensitivity of diatom taxa
1525 from Yakutian lakes (north-eastern Siberia) to electrical conductivity and other environmental
1526 variables, *Polar Research*, 37, 10.1080/17518369.2018.1485625, 2018.
- 1527 Petschick, R., Kuhn, G., and Gingele, F.: Clay mineral distribution in surface sediments of the South
1528 Atlantic: sources, transport, and relation to oceanography, *Marine Geology*, 130, 203-229, 1996.
- 1529 Pillot, H. K. M. M.: Chironomidae Larvae of the Netherlands and adjacent lowlands: biology and
1530 ecology of the chironomini, KNNV publishing, 2009.
- 1531 Puusepp, L., and Punning, J. M.: Spatio-temporal variability of diatom assemblages in surface
1532 sediments of Lake Peipsi, *Journal of Great Lakes Research*, 37, 33-40, 10.1016/j.jglr.2010.11.018,
1533 2011.
- 1534 QGIS-Team: QGIS geographic information system, Open Source Geospatial Foundation Project,
1535 2016.
- 1536 R Core Team: R: A language and environment for statistical computing. R Foundation for Statistical
1537 Computing, Vienna, Austria, 2012. ISBN 3-900051-07-0, 2012.

- 1538 Raposeiro, P. M., Saez, A., Giralt, S., Costa, A. C., and Goncalves, V.: Causes of spatial distribution
1539 of subfossil diatom and chironomid assemblages in surface sediments of a remote deep island lake,
1540 *Hydrobiologia*, 815, 141-163, 10.1007/s10750-018-3557-4, 2018.
- 1541 Round, F. E., Crawford, R. M., and Mann, D. G.: *The Diatoms. Biology & Morphology of the Genera*,
1542 Cambridge University Press, Cambridge, 747 pp., 1990.
- 1543 Rühland, K., Priesnitz, A., and Smol, J. P.: Paleolimnological evidence from diatoms for recent
1544 environmental changes in 50 lakes across Canadian arctic treeline, *Arctic Antarctic and Alpine*
1545 *Research*, 35, 110-123, 10.1657/1523-0430(2003)035[0110:pefdfjr]2.0.co;2, 2003.
- 1546 Rühland, K., Paterson, A. M., and Smol, J. P.: Hemispheric-scale patterns of climate-related shifts in
1547 planktonic diatoms from North American and European lakes, *Global Change Biology*, 14, 2740-
1548 2754, 10.1111/j.1365-2486.2008.01670.x, 2008.
- 1549 Rühland, K. M., Paterson, A. M., and Smol, J. P.: Lake diatom responses to warming: reviewing the
1550 evidence, *Journal of Paleolimnology*, 1-35, DOI: 10.1007/s10933-015-9837-3, 2015.
- 1551 Rundqvist, D. V., and Mitrofanov, F. P.: *Precambrian Geology of the USSR*, 1-528 pp., 1993.
- 1552 Ryves, D., Juggins, S., Fritz, S., and Battarbee, R.: Experimental diatom dissolution and the
1553 quantification of microfossil preservation in sediments, *Palaeogeography Palaeoclimatology*
1554 *Palaeoecology*, 172, 99-113, 2001.
- 1555 Schleusner, P., Biskaborn, B. K., Kienast, F., Wolter, J., Subetto, D., and Diekmann, B.: Basin
1556 evolution and palaeoenvironmental variability of the thermokarst lake El'gene-Kyuele, Arctic Siberia,
1557 *Boreas*, 44, 216-229, 10.1111/bor.12084, 2015.
- 1558 Schuur, E. A. G., McGuire, A. D., Schadel, C., Grosse, G., Harden, J. W., Hayes, D. J., Hugelius, G.,
1559 Koven, C. D., Kuhry, P., Lawrence, D. M., Natali, S. M., Olefeldt, D., Romanovsky, V. E., Schaefer,
1560 K., Turetsky, M. R., Treat, C. C., and Vonk, J. E.: Climate change and the permafrost carbon
1561 feedback, *Nature*, 520, 171-179, 10.1038/nature14338, 2015.
- 1562 Self, A. E., Brooks, S. J., Birks, H. J. B., Nazarova, L., Porinchu, D., Odland, A., Yang, H., and Jones,
1563 V. J.: The distribution and abundance of chironomids in high-latitude Eurasian lakes with respect to
1564 temperature and continentality: development and application of new chironomid-based climate-
1565 inference models in northern Russia, *Quaternary Science Reviews*, 30, 1122-1141,
1566 10.1016/j.quascirev.2011.01.022, 2011.
- 1567 Semenov, S. G.: Current state of ichthyofauna of Lake Bolshoe Toko, South of Russia-Ecology
1568 Development, 13, 32-42, 2018.
- 1569 Shahgedanova, M.: Climate at Present and in the Historical Past, in: *The Physical Geography of*
1570 *Northern Eurasia*, edited by: Shahgedanova, M., Oxford University Press, Oxford, 70-102, 2002.
- 1571 Smol, J. P.: The Statospore of *Mallomonas Pseudocoronata* (Mallomonadaceae, Chrysophyceae),
1572 *Nord J Bot*, 4, 827-831, DOI 10.1111/j.1756-1051.1984.tb02014.x, 1984.
- 1573 Smol, J. P., Charles, D. F., and Whitehead, D. R.: Mallomonadacean Microfossils Provide Evidence
1574 of Recent Lake Acidification, *Nature*, 307, 628-630, DOI 10.1038/307628a0, 1984.
- 1575 Smol, J. P., and Boucherle, M. M.: Postglacial changes in algal and cladoceran assemblages in Little
1576 Round Lake, Ontario, *Archiv Fur Hydrobiologie*, 103, 25-49, 1985.
- 1577 Smol, J. P.: Chrysophycean microfossils in paleolimnological studies, *Palaeogeography*
1578 *Palaeoclimatology Palaeoecology*, 62, 287-297, 1988a.

- 1579 Smol, J. P.: Paleoclimate proxy data from freshwater arctic diatoms, *Verh. Internat. Verein. Limnol.*,
1580 23, 837-844, 1988b.
- 1581 Smol, J. P., Wolfe, A. P., Birks, H. J. B., Douglas, M. S. V., Jones, V. J., Korhola, A., Pienitz, R.,
1582 Rühland, K., Sorvari, S., Antoniades, D., Brooks, S. J., Fallu, M. A., Hughes, M., Keatley, B. E.,
1583 Laing, T. E., Michelutti, N., Nazarova, L., Nyman, M., Paterson, A. M., Perren, B., Quinlan, R.,
1584 Rautio, M., Saulnier-Talbot, E., Siitonen, S., Solovieva, N., and Weckstrom, J.: Climate-driven
1585 regime shifts in the biological communities of arctic lakes, *Proceedings of the National Academy of
1586 Sciences of the United States of America*, 102, 4397-4402, 10.1073/pnas.0500245102, 2005.
- 1587 Smol, J. P., and Douglas, M. S. V.: Crossing the final ecological threshold in high Arctic ponds,
1588 *Proceedings of the National Academy of Sciences of the United States of America*, 104, 12395-
1589 12397, 10.1073/pnas.0702777104, 2007.
- 1590 Sobakina, I., and Solomonov, N.: To the study of zooplankton of Lake Bolshoe Toko, *International
1591 Journal of applied and fundamental research*, 8, 180-182, 2013.
- 1592 Solovieva, N., Klimaschewski, A., Self, A. E., Jones, V. J., Andrén, E., Andreev, A. A., Hammarlund,
1593 D., Lepskaya, E. V., and Nazarova, L.: The Holocene environmental history of a small coastal lake
1594 on the north-eastern Kamchatka Peninsula, *Global and Planetary Change*, 134, 55-66, 2015.
- 1595 Specziar, A., Arva, D., Toth, M., Mora, A., Schmera, D., Varbiro, G., and Eros, T.: Environmental and
1596 spatial drivers of beta diversity components of chironomid metacommunities in contrasting freshwater
1597 systems, *Hydrobiologia*, 819, 123-143, 10.1007/s10750-018-3632-x, 2018.
- 1598 Stewart, K. A., and Lamoureux, S. F.: Seasonal and microhabitat influences on diatom assemblages
1599 and their representation in sediment traps and surface sediments from adjacent High Arctic lakes:
1600 Cape Bounty, Melville Island, Nunavut, *Hydrobiologia*, 683, 265-286, 10.1007/s10750-011-0965-0,
1601 2012.
- 1602 Stief, P., Nazarova, L., and de Beer, D.: Chimney construction by *Chironomus riparius* larvae in
1603 response to hypoxia: microbial implications for freshwater sediments, *Journal of the North American
1604 Benthological Society*, 24, 858-871, 2005.
- 1605 Subetto, D. A., Nazarova, L. B., Pestryakova, L. A., Syrykh, L. S., Andronikov, A. V., Biskaborn, B.,
1606 Diekmann, B., Kuznetsov, D. D., Sapelko, T. V., and Grekov, I. M.: Paleolimnological studies in
1607 Russian northern Eurasia: A review, *Contemporary Problems of Ecology*, 10, 327-335,
1608 10.1134/s1995425517040102, 2017.
- 1609 Swann, G. E. A., Leng, M. J., Sloane, H. J., Maslin, M. A., and Onodera, J.: Diatom oxygen isotopes:
1610 Evidence of a species effect in the sediment record, *Geochemistry Geophysics Geosystems*, 8,
1611 10.1029/2006gc001535, 2007.
- 1612 Syrykh, L. S., Nazarova, L. B., Herzsuh, U., Subetto, D. A., and Grekov, I. M.: Reconstruction of
1613 palaeoecological and palaeoclimatic conditions of the Holocene in the south of the Taimyr according
1614 to an analysis of lake sediments, *Contemporary Problems of Ecology*, 10, 363-369,
1615 10.1134/s1995425517040114, 2017.
- 1616 ter Braak, C. J. F., and Prentice, I. C.: A theory of gradient analysis, in: *Advances in ecological
1617 research*, Elsevier, 271-317, 1988.
- 1618 ter Braak, C. J. F.: Ordination, in: *Data analysis in community and landscape ecology*, Cambridge
1619 University Press, 91-274, 1995.
- 1620 ter Braak, C. J. F., and Šmilauer, P.: *Canoco reference manual and user's guide: software for
1621 ordination*, version 5.0, Microcomputer power, 2012.

- 1622 Tjallingii, R., Rohl, U., Kolling, M., and Bickert, T.: Influence of the water content on X-ray
1623 fluorescence core-scanning measurements in soft marine sediments, *Geochemistry Geophysics*
1624 *Geosystems*, 8, Q02004
1625 10.1029/2006gc001393, 2007.
- 1626 Valiranta, M., Weckstrom, J., Siitonen, S., Seppa, H., Alkio, J., Juutinen, S., and Tuittila, E. S.:
1627 Holocene aquatic ecosystem change in the boreal vegetation zone of northern Finland, *Journal of*
1628 *Paleolimnology*, 45, 339-352, 10.1007/s10933-011-9501-5, 2011.
- 1629 Vemeaux, V., and Aleya, L.: Spatial and temporal distribution of chironomid larvae (Diptera:
1630 Nematocera) at the sediment—water interface in Lake Abbaye (Jura, France), in: *Oceans, Rivers*
1631 *and Lakes: Energy and Substance Transfers at Interfaces*, Springer, 169-180, 1998.
- 1632 Virgo, D.: Partition of Strontium between Coexisting K-Feldspar and Plagioclase in Some
1633 Metamorphic Rocks, *The Journal of Geology*, 76, 331-346, 10.1086/627332, 1968.
- 1634 Vogel, H., Wessels, M., Albrecht, C., Stich, H. B., and Wagner, B.: Spatial variability of recent
1635 sedimentation in Lake Ohrid (Albania/Macedonia), *Biogeosciences*, 7, 3333-3342, 2010.
- 1636 Voigt, C.: Data report: semiquantitative determination of detrital input to ACEX sites based on bulk
1637 sample X-ray diffraction data, in: *Proceedings of the Integrated Ocean Drilling Program, Volume 302*,
1638 edited by: Backman, J., Moran, K., McInroy, D.B., Mayer, L.A., and the Expedition 302 Scientists,
1639 Edinburgh, 2009.
- 1640 Walker, I. R., and Mathewes, R. W.: Early postglacial chironomid succession in southwestern British
1641 Columbia, Canada, and its paleoenvironmental significance, in: *Paleolimnology and the*
1642 *Reconstruction of Ancient Environments*, Springer, 147-160, 1990.
- 1643 Walker, I. R., Levesque, A. J., Cwynar, L. C., and Lotter, A. F.: An expanded surface-water
1644 palaeotemperature inference model for use with fossil midges from eastern Canada, *Journal of*
1645 *Paleolimnology*, 18, 165-178, 1997.
- 1646 Wang, L., Rioual, P., Panizzo, V. N., Lu, H., Gu, Z., Chu, G., Yang, D., Han, J., Liu, J., and Mackay,
1647 A. W.: A 1000-yr record of environmental change in NE China indicated by diatom assemblages from
1648 maar lake Erlongwan, *Quaternary Research*, 78, 24-34, 10.1016/j.yqres.2012.03.006, 2012a.
- 1649 Wang, Q., Yang, X. D., Hamilton, P. B., and Zhang, E. L.: Linking spatial distributions of sediment
1650 diatom assemblages with hydrological depth profiles in a plateau deep-water lake system of
1651 subtropical China, *Fottea*, 12, 59-73, 2012b.
- 1652 Wang, R., Zhang, Y., Wuennemann, B., Biskaborn, B. K., Yin, H., Xia, F., Zhou, L., and Diekmann,
1653 B.: Linkages between Quaternary climate change and sedimentary processes in Hala Lake, northern
1654 Tibetan Plateau, China, *Journal of Asian Earth Sciences*, 107, 140-150,
1655 10.1016/j.jseaes.2015.04.008, 2015.
- 1656 Weltje, G. J., and Tjallingii, R.: Calibration of XRF core scanners for quantitative geochemical logging
1657 of sediment cores: Theory and application, *Earth and Planetary Science Letters*, 274, 423-438,
1658 10.1016/j.epsl.2008.07.054, 2008.
- 1659 Wiederholm, T.: Chironomidae of Holarctic region: keys and diagnoses. Part 1, *Larvae Entomol*
1660 *Scand Suppl*, 19, 1-457, 1983.
- 1661 Wischniewski, J., Mackay, A. W., Appleby, P. G., Mischke, S., and Herzs Schuh, U.: Modest diatom
1662 responses to regional warming on the southeast Tibetan Plateau during the last two centuries,
1663 *Journal of Paleolimnology*, 46, 215-227, 10.1007/s10933-011-9533-x, 2011.

- 1664 Wolfe, A.: Spatial patterns of modern diatom distribution and multiple paleolimnological records from
1665 a small arctic lake on Baffin Island, Arctic Canada, *Canadian Journal of Botany-Revue Canadienne*
1666 *De Botanique*, 74, 435-449, 1996.
- 1667 Yang, H., Flower, R. J., and Battarbee, R. W.: Influence of environmental and spatial variables on the
1668 distribution of surface sediment diatoms in an upland loch, Scotland, *Acta Botanica Croatica*, 68,
1669 367-380, 2009.
- 1670 Yang, L. W., Chen, S. Y., Zhang, J., Yu, S. Y., and Deng, H. G.: Environmental factors controlling the
1671 spatial distribution of subfossil Chironomidae in surface sediments of Lake Dongping, a warm
1672 temperate lake in North China, *Environmental Earth Sciences*, 76, 10.1007/s12665-017-6858-4,
1673 2017.
- 1674 Zhirkov, I., Trofimova, T., Zhirkov, K., Pestryakova, L., Sobakina, I., and Ivanov, K.: Current
1675 geoecological state of Lake Bolshoe Toko, *International Journal of applied and fundamental*
1676 *research*, 8, 208-213, 2016.
- 1677 Zinchenko, T. D., Gladyshev, M. I., Makhutova, O. N., Sushchik, N. N., Kalachova, G. S., and
1678 Golovatyuk, L. V.: Saline rivers provide arid landscapes with a considerable amount of biochemically
1679 valuable production of chironomid (Diptera) larvae, *Hydrobiologia*, 722, 115-128, 2014.
1680